Parkin-phosphoubiquitin complex reveals a cryptic ubiquitin binding site required for RBR ligase activity

Atul Kumar[1], Viduth K Chaugule[1], Tara E C Condos[2], Kathryn R Barber[2], Clare Johnson[1], Rachel Toth[1], Ramasubramanian Sundaramoorthy[3], Axel Knebel[1], Gary S Shaw[2] and Helen Walden[1,*]

[1]MRC Protein Phosphorylation and Ubiquitylation Unit, College of Life Sciences University of Dundee, Dundee, UK

[2]Department of Biochemistry, Schulich School of Medicine and Dentistry, Universtiy of Western Ontario, London, ON, Canada

[3]Centre for Gene Regulation and Expression, College of Life Sciences, University of Dundee, Dundee, UK

* Corresponding author. Tel: +44 1382 384109; E-mail: h.walden@dundee.ac.uk

Abstract

RING-BETWEENRING-RING (RBR) E3 ligases are a class of ubiquitin ligases distinct from RING or HECT E3 ligases. An important RBR is Parkin, mutations in which lead to early onset hereditary Parkinsonism. Parkin and other RBRs share a catalytic RBR module, but are usually autoinhibited and activated via distinct mechanisms. Recent insights into Parkin regulation predict large, unknown conformational changes during activation of Parkin. However, current data on active RBRs are in the absence of regulatory domains. Therefore, how individual RBRs are activated, and whether they share a common mechanism remains unclear. We now report the crystal structure of a human Parkin-phosphoubiquitin complex, which shows that phosphoubiquitin binding induces a movement in the IBR domain to reveal a cryptic ubiquitin binding site. Mutation of this site negatively impacts on Parkin's activity. Furthermore, ubiquitin binding promotes cooperation between Parkin molecules, suggesting a role for interdomain association in RBR ligase mechanism.

Introduction

Parkinson's Disease (PD) is a neurodegenerative disorder characterised by the progressive loss of dopaminergic neurons, bradykinesia and tremor [1]. Although primarily a sporadic disorder, mutations in several genes are associated with different Parkinsonism syndromes [2], including the genes *PARK2* and *PARK6* which lead to autosomal recessive juvenile Parkinsonism (ARJP) [3,4]. *PARK2* and *PARK6* encode Parkin E3 Ubiquitin ligase and PTEN-induced kinase (PINK-1), respectively, and maintain mitochondrial homeostasis [5-8]. In addition to its role in mitochondrial protein control, Parkin also regulates protein degradation and induces aggresome formation by K63-linked ubiquitination [9-11].

Parkin belongs to the RBR E3 ubiquitin ligase family, characterised by a RING domain (RING1) followed by an 'in-between RING' (IBR) domain and a catalytic domain (RING2 or Rcat [12]). RING1 is structurally similar to canonical RING-type E3 ligases, and shares the function of binding to E2 ubiquitin conjugating enzymes. In contrast, RING2(Rcat) adopts a linear zinc-binding fold [13,14] and possesses a catalytic cysteine capable of forming a thioester bond with activated ubiquitin [13,15-19]. The linking 'IBR' domain adopts the same fold as the RING2(Rcat) [20], however its functional role remains unclear. RBR ligases contain additional domains outwith the RBR module. Parkin has an N-terminal ubiquitin-like domain (UBL), which shares 65% homology with ubiquitin, and a zinc-binding RING0 or unique parkin domain (UPD) [21]. Parkin adopts an autoinhibited conformation mediated by multiple domain-domain interactions [22-26]. This autoinhibition is released by PINK1-dependent phosphorylation of ubiquitin and the UBL domain of Parkin, leading to activation of Parkin [27-32]. Additional RBR ligase family members include HOIP, which is a subunit of the linear ubiquitin chain assembly complex (LUBAC) [33], and the human

homologue of Ariadne, HHARI [34]. The catalytic activity of HOIP is also regulated through autoinhibition, mediated by its UBA domain, which interacts with the other subunits of LUBAC, HOIL-1L and SHARPIN to activate HOIP [17,33,35,36]. HHARI is also autoinhibited, mediated through its Ariadne domain [37]. HHARI activation requires interaction of the UBA domain of HHARI with NEDD8 [38,39]. Thus our current understanding of Parkin and other RBRs suggests distinct modes of regulation. In the case of Parkin, we and others have shown that the binding of phosphoubiquitin, leads to Parkin activation via removal of the inhibitory effect of the Ubl domain [23,24,40-43]. However, all the structural insights into Parkin are in the context of the autoinhibited state [23-25], or in the absence of the regulatory Ubl domain [16,25,26,43]. Insights into HHARI are also based on an inactive conformation [37]. Recent insights into the catalytic mechanism of the RBR family have come from structural and physical analyses of HOIP [14,44]. The crystal structure of the catalytic RING2-Like (RING2L) or Rcat domain of HOIP in complex with ubiquitin revealed how linear chains are assembled [14], while a recent complex of the RBR module of HOIP in complex with a charged E2~ubiquitin conjugate revealed a series of allosteric ubiquitin-binding sites coupled to a swapped dimer of the RING2L(Rcat) domain between RBR molecules[44]. Furthermore, the RING2(Rcat) of HHARI has a ubiquitin binding site important for E2~ubiquitin recruitment [45], and the RING1 of HHARI supports an open conformation of the E2~ubiquitin conjugate. In contrast a structure of the RING0-RBR (R0RBR) domains from *Pediculus humanus corporis* Parkin, in complex with phosphoubiquitin does not show domain swapping between RBR modules, but rather revealed a conformational change in the IBR domain upon phosphoubiquitin binding [43]. Our current understanding is derived from snapshots of individual domains of large multidomain complexes. However, how RBR ligases

function in the context of their regulatory domains remains unclear, and whether they share a universal catalytic mechanism remains unclear.

We report here the crystal structures of activated human Parkin (UblR0RBR), and a phosphomimic Parkin (S65DUblR0RBR), in complex with phosphoubiquitin, at 2.7 and 2.6 Å resolution respectively. All Parkin domains are present, and in contrast to earlier predictions of large conformational rearrangements upon activation, the Parkin structures reveal subtle, local changes that result in a series of cryptic ubiquitin or ubiquitin-like binding regions that are essential for Parkin function. We find an essential role of the IBR domain in ubiquitin recruitment and Parkin activity. Furthermore, comparative analyses with the HOIP and HHARI modules reveals common ubiquitin or ubiquitin-like binding sites. In particular, comparison with the RBR of HOIP suggests a potential unifying mechanism of cooperation between multiple RBR modules in the mechanism of ubiquitin ligase activity.

Results

Crystal structure of UBLR0RBR Parkin in complex with pUb reveals activated state of Parkin

Previous studies by ourselves and others suggest that binding of phosphoubiquitin to Parkin relieves the autoinhibition by the UBL domain. Consistent with this, the UBL domain displays weaker binding to the R0RBR fragment of Parkin in *trans* upon phosphoubiquitin binding [23,24,40-43,46]. In order to understand the allosteric regulation by phosphoubiquitin, we crystallised a complex of Parkin UBLR0RBR (Δ84-143) with a phosphoubiquitin (pUb) suicide probe (pUb3BR, pUb bromopropylamine). To enable the formation of stable, well diffracting crystals, we generated a covalent Parkin-pUb complex by ligating the pUb3BR probe to a cysteine

106 residue on the surface of Parkin. The cysteine was provided by mutating Gln347, as
107 described previously [43]. The structure of activated Parkin was refined to 2.7 Å (Table
108 1), with good geometry and refinement statistics. The crystal structure of the Parkin-
109 pUb complex reveals the activated state of Parkin, containing all 5 domains of Parkin
110 UBL, RING0, RING1-IBR-RING2(Rcat) and pUb (Fig 1a). In the asymmetric unit,
111 UBL, RING1-IBR-RING2(Rcat) are contributed from one molecule whereas RING0
112 and pUb are from another molecule, with the biological unit via symmetry related
113 molecules (Supp Fig 1a). Comparison of the activated state of Parkin-pUb with the
114 apo, inactive UBLR0RBR structure [23] shows that although some small
115 rearrangements occur, the UBL-RING1 interface, primarily formed by between β3
116 and β5 of the UBL domain, and helix H1 of the RING1 domain, remains largely
117 intact in the presence of phosphoubiquitin (Fig 1b). The largest structural
118 rearrangement upon activation is the movement of the IBR domain. Helix H3 of the
119 RING1 domain straightens, leading to global movement of the IBR domain
120 (henceforth this helix is referred to as H3-IBR), and creating a void between the UBL
121 and IBR domains. This straightening of the H3-IBR helix is also observed in the
122 insect Parkin R0RBR complex with pUb that lacks the UBL domain [43]. In the apo
123 structure this UBL-IBR interface is formed primarily through interactions of His11 of
124 the UBL domain with Lys369, Glu370 of the IBR domain, and surrounding residues,
125 and these interactions are lost in the phosphoubiquitin-bound complex.
126 Phosphorylation of the UBL domain by PINK-1 has been shown to weaken
127 association of the UBL domain with R0RBR Parkin [23,24,42,46,47]. Therefore, we
128 wondered whether inclusion of a negative charge at Ser65 to mimic phosphorylation
129 would lead to displacement of the UBL domain in presence of pUb. To test this, we
130 crystallised a covalent complex of S65D-UBLR0RBR Parkin with the pUb suicide

probe. In this structure, refined to 2.6 Å resolution, the S65D-UBL domain remains associated with RING1 (Supp Fig.1b). However, there are local conformational rearrangements between UBLR0RBR/S65SD-UBLR0RBR in complex with pUb and the apo structure of UBLR0RBR. In the apo structure of UBLR0RBR, residues 383-390, part of the tether that connects the IBR domain to the Repressor Element of Parkin (REP) are disordered [23,25]. In contrast, this tether, residues 387-390, is ordered and traceable in the WT Parkin-pUb complex, with Arg392 pointing towards the disordered side-chain of Lys48 in the UBL domain. This Arg392-Lys48 creates an electrostatic repulsion, while Gln389 and Tyr391 cement the association of the UBL-RING1 interface, resulting in flexibility of the 62-65 loop in the UBL domain (Supp Fig 1b). Upon inclusion of a negative charge at position 65, Tyr391 relocates from the UBL-RING1 interface, resulting in disorder of the IBR-REP tether and ordering of the 62-65 loop in the UBL domain (Supp Fig 1c). We wondered whether mutation of these residues would enable the UBL domain to bind ΔUBL-Parkin in the presence of pUb. In the absence of pUb, the UBL domain associates with ΔUBL-Parkin (80-465) with a dissociation constant (Kd) in the low micromolar range [22-24,43] (Supp Fig 1d). The presence of pUb blocks the UBL interaction with ΔUBL- Parkin (Supp Fig 1d). Gln389Ala, Tyr391Ala and Arg392Ala mutation in ΔUBL-Parkin does not permit UBL re-association in the presence of pUb (Supp Fig 1d). Given that the structures clearly show the UBL-RING1 interface persists in the presence of pUb, we wondered whether the loss of association in solution could be due to a weakened UBL-IBR interface (Fig 1B), rather than UBL-RING1 interface. To test this, we expressed and purified human Parkin lacking the IBR domain, and measured the interaction of the UBL domain with Parkin, using isothermal titration calorimetry (ITC). The UBL domain does not associate with ΔUBL-ΔIBR (80-329,383-465) (Fig 1c). In order to

understand the role of the IBR domain we assayed this mutant for E3 ligase activity. ΔUBL-Parkin is active, both in the absence and presence of phosphoubiquitin (Fig 1d). In contrast, deletion of the IBR domain in ΔUBL-Parkin leads to complete loss of Parkin activity, which cannot be rescued by the addition of pUb. It is a possibility that removal of the IBR domain results in a constrained version of Parkin that lacks the flexibility needed for maintenance of its catalytic domains. In order to rule this possibility out, we purified ΔUBL-ΔIBR containing a 10-residue (Gly-Thr-Ser-Gly-Thr-Ser-Gly-Ser-Ala-Ser) (ΔUBL-ΔIBRxL10) linker to span the 28 Å distance required, and assayed for ubiquitination activity (Fig 1d). These constructs lacking the IBR domain are folded, monodisperse and migrate at the expected molecular weight, consistent with folded proteins. In contrast to wild-type and ΔUBL-Parkin, both ΔUBL-ΔIBR and ΔUBL-ΔIBRxL10 Parkin lack ubiquitination activity, even in the presence of phosphoubiquitin. Interestingly, the surface of the UBL domain when phosphorylated would result in repulsion with the negatively charged surface of IBR, supporting a weakened UBL-IBR interaction (Supp Fig 1e). The observation that the UBL domain and pUb both interact with IBR, on opposite sides, could explain the competitive mode of binding to Parkin that has previously been observed [23,24]. Taken together, these results show that activation of Parkin by phosphoubiquitin binding involves loosening of the UBL-IBR interface, caused by a straightening of the H3-IBR helix. Furthermore, these experiments show that the association of the UBL domain with the rest of Parkin depends upon the presence of the IBR domain in addition to the more extensive RING1 surface, and that Parkin activity requires an intact IBR domain.

Parkin activation exposes ubiquitin or ubiquitin-like binding surfaces that are essential for Parkin activity

The straightening of the H3-IBR helix caused by phosphoubiquitin binding results in a void being created between the UBL and IBR domains (Supp Fig 2a). Intriguingly, analysis of the crystal packing of activated Parkin reveals that this void is occupied by the UBL domain of another molecule of Parkin (Supp Fig 2b). The UBL domain of Parkin shares 65% sequence similarity with ubiquitin. We therefore wondered whether the void created by the loosening of the UBL-IBR interaction, occupied in our crystal structures by the UBL domain of a second molecule of Parkin, could accommodate ubiquitin. To explore this idea, we modelled ubiquitin into the void (Fig 2a). This arrangement reveals potential surfaces on Parkin that could interact with ubiquitin, referred to as Ubiquitin Binding Region (UBR) 1,2, and 3, respectively (Fig 2). UBR1 is contributed by the UBL domain of Parkin, mediated by His11, Phe13, Arg33, Gln34 (Fig 2b). Mutation of UBR1 residues on Parkin results in a minor reduction in ubiquitin chain formation, but no observable decrease in substrate ubiquitination, in this case Miro1 (Fig 2b). UBR2 and UBR3 are formed on the straightened helix (H3) of RING1 and the IBR of Parkin, respectively. The potential ubiquitin binding surfaces are mediated by Arg275, Gln317, Tyr318, Glu321 on H3 of RING1, and Arg334 and Pro335 of the β-hairpin on IBR (Fig 2c). Mutations in UBR2 (R275A, Y318A, E321A) and UBR3 (R334A) result in loss of E3 ligase activity, both in ubiquitin chain formation and Miro1 ubiquitination (Fig 2c). Therefore, UBR2 and UBR3, but not UBR1, are important for Parkin activity. In order to further clarify which regions of activated Parkin interact with ubiquitin, we performed NMR chemical shift perturbation experiments of the R0RBR fragment of Parkin in complex with pUb (Fig 2d). Upon addition of unlabelled Ub to the R0RBR-

pUb complex it was clear that the IBR domain was a major site of interaction. The largest chemical shift changes occur for residues G329-R334 of the β-hairpin and the adjoining loop (G361-A363, R366) of the IBR domain. Changes were also observed in the straightened helix (H3) of RING (R314, V324) near those observed in the crystal structure. However, several of these resonances are broadened by pUb binding and are therefore difficult to visualise in the NMR spectra. Nevertheless, this analysis shows a large ubiquitin interaction surface in activated Parkin that is consistent with that for UBR2 and UBR3 sites predicted from the crystal packing analyses. These findings suggest a role for ubiquitin (or ubiquitin-like protein) binding at surfaces exposed upon pUb binding in the regulation of Parkin activity. Consistent with this, a recent study shows that modification of the IBR domain at Lys349 and Lys369 by the ubiquitin-like protein ISG15, positively regulates Parkin activity [48]. Interestingly, Lys349 is also a target of Parkin autoubiquitination activity [13]. Therefore, we wondered whether Parkin modification by ubiquitin can influence Parkin activity. To explore this possibility, we generated a covalently linked Parkin carrying a ubiquitin chain (UBLR0RBR347Cys~pUb-M1-$(UBS65A)_3$, to mimic polyubiquitinated Parkin. In comparison with UBLR0RBR347Cys~pUb or providing pUb to UBLR0RBR in *trans*, UBLR0RBR347Cys~pUb-M1-$(UBS65A)_3$ activity is dramatically enhanced (Supp Fig 2c). Taken together, these data suggest an important role for the displacement of the UBL-IBR interface, revealing that modification of the IBR, phosphorylation of Ser65 in the UBL-IBR interface, and pUb binding to the IBR domain all contribute to the creation of a ubiquitin/ubl binding region, and that ubiquitin binding stimulates Parkin activity.

The UBL-IBR ubiquitin binding site recruits the donor ubiquitin

230 The arrangement of phosphoubiquitin of one molecule of Parkin, and the UBL
231 domain of a second molecule, is reminiscent of the activator ubiquitin and donor
232 ubiquitin recently described in the structure of the RBR of HOIP in complex with a
233 charged E2 [44] (Fig 3a). Furthermore, UbcH7 interaction with phosphorylated Parkin is
234 enhanced 20 fold by the addition of phosphoubiquitin and charging of the E2 with
235 ubiquitin [23,49]. Thus we wondered whether the ubiquitin binding site created from the
236 activation of Parkin by phosphoubiquitin could accommodate the charged
237 E2~ubiquitin conjugate. To test this, we measured UbcH7 or UbcH7~ubiquitin
238 interaction with phosphoparkin (pParkin) or a UBR2 mutant pParkinE321A, in the
239 presence of pUb. ITC experiments show a similar affinity of pParkin or
240 pParkinE321A for UbcH7 (Kd of 19 and 23.5 μM respectively) in the presence of
241 pUb, suggesting that mutation of the ubiquitin binding region of Parkin does not
242 interfere with E2 binding (Fig 3b). In contrast, while phosphoParkin binds to
243 UbcH7~ubiquitin with a 30-fold higher affinity, this enhanced binding is diminished
244 for phosphoParkinE321A (~2.5 fold) (Fig 3b). In addition, size exclusion
245 chromatography of these complexes reveals that mutation of E321 to alanine
246 abolishes formation of the phosphoParkin UbcH7~Ub complex in the presence of
247 phosphoubiquitin (Supp Fig 3a). We ruled out the possibility that mutation of E321
248 leads to loss of phosphoubiquitin binding by ITC measurement (Supp Fig 3b). These
249 data suggest that the ubiquitin carried by charged E2 binds at the UBR regions in
250 activated Parkin. Previous studies have shown that when the only source of ubiquitin
251 is phosphoubiquitin, Parkin cannot catalyse ubiquitin chains [49,50]. However, UbcH7
252 can be charged with pUb [50]. Furthermore, measurements of Parkin fragments
253 interacting with either ubiquitin or pUb showed a similar isotherm profile, but with
254 much tighter binding to pUb [23]. Both these observations suggest that the pUb-binding

pocket on the surface of Parkin is the dominant ubiquitin binding site. Therefore we wondered whether loading of E2 with pUb redirects the conjugate to the pUb binding site on the Parkin, rather than going to the donor ubiquitin binding site. To test this, we "activated" Parkin using either pUb, or UbcH7 charged with pUb (Ubch7~pUb). Interestingly, UbcH7~pUb, but not UbcH7~ubiquitin, activates Parkin to a similar extent as pUb alone (Fig 3c). Taken together, these data suggest that the cryptic ubiquitin binding site created between the UBL-IBR domains upon Parkin activation, recruits the donor ubiquitin as carried by the E2.

Cooperation between multiple Parkin molecules promotes ubiquitin transfer

Using the position of the UBL domain, the HOIP RBR/E2~Ub structure, and the chemical shift perturbations on Parkin as guides, we modelled an activated Parkin-donor ubiquitin complex (Supp Fig 4a). In the model, with only one molecule of Parkin, it is difficult to envision how the E2 of the E2~Ub conjugate would reach the proposed E2 binding site at the base of the RING1. In addition, it is difficult to determine how the ubiquitin would reach the catalytic cysteine in the RING2(Rcat). Indeed, despite many efforts to understand how the catalytic cysteine in the RING2(Rcat) domain mechanistically directs Parkin activity, previous Parkin structures show that the Cys431 of the RING2(Rcat) domain is ~35 Å away (using the sulfur of Cys431, and the side-chain oxygen of Thr240 as the reference points) from the predicted E2 binding site on RING1 [25]. Furthermore, multiple groups have reported that Cys431 is occluded by RING0 [16,25,26]. In our crystal structure of the Parkin-pUb complex, one molecule of activated Parkin accommodates a UBL domain from a neighbouring molecule, which we model as donor ubiquitin. This modelled donor ubiquitin packs against the catalytic RING2(Rcat) domain of a neighbouring

Parkin molecule (Fig 4a). This quarternary arrangement of Parkin molecules can also accommodate an E2, with proposed interactions with the RING1 and REP of molecule 2, satisfying observed E2 interaction sites in HOIP and HHARI [44,45] (Fig 4a). Therefore, we wondered whether the UBR2 donor ubiquitin binding site would affect the loading on ubiquitin onto the catalytic cysteine (C431). In order to test this, we designed an *in vitro* assay that evaluates the transfer of donor ubiquitin from the E2 to the RBR catalytic residue. First, we generated a Parkin RING2(Rcat) mutant, able to trap the catalytic Parkin~Ub intermediate [13,17], referred to as R0RBR^{CH}. This species has a serine in place of the catalytic cysteine (C431S) and a His433Ala mutation in order to trap an ester-bound ubiquitin and impede any subsequent discharge. This R0RBR^{CH} Parkin species can be charged with ubiquitin and was sensitive to sodium hydroxide hydrolysis thus confirming the RING2(Rcat)-ubiquitin ester link. The addition of phosphoubiquitin in this setup greatly enhances the RING2(Rcat) charging by around 7-fold while a catalytic Cys431Ala mutant (R0RBR C431A) Parkin cannot be charged with ubiquitin in either scenario (Fig 4b). We then generated a UBR2 patch mutant of Parkin in this background, R0RBR^{CH} E321A. In contrast to R0RBR^{CH}, this mutant is defected in ubiquitin charging even in the presence of phosphoubiquitin (26-fold less). Finally, a combined mutant of the phosphoubiquitin patch and the UBR2 patch (R0RBR^{CH} H302A+E321A) was drastically reduced (60-fold less) in ubiquitin charging of the RING2(Rcat) (Fig 4b). Recent studies have suggested a physiological role for self-association of Parkin molecules. For example, in 2013, two independent studies reported the observation that catalytically compromised Parkin (C431 mutants) could not translocate to the mitochondria after PINK1 activation [15,19]. However, co-expression of C431 mutant Parkin with either wild-type Parkin, or other mutations including the R275W that

would affect the UBR2 binding site, could rescue this translocation defect. These observations raise the possibility of cooperation between Parkin molecules. We have demonstrated that mutation of the donor ubiquitin binding site UBR2 in Parkin results in loss of Miro1 ubiquitination (Fig 2c). Thus we wondered whether a constitutively phosphoubiquitin-bound form of Parkin could support the activity of otherwise inactive Parkin, in this case phosphoParkinE321A. To test this, we took the crystallised species of Parkin UblR0RBR covalently linked to phosphoubiquitin, and titrated it into phosphoParkinE321A (Fig 4c). We find that wild-type phosphoParkin can ubiquitinate Miro1 (Fig 4c). Addition of UblR0RBR, or UblR0RBR covalently complexed with pUb does not further enhance this activity. In contrast, phosphoParkinE321A is defective in Miro1 ubiquitination (Fig 4c). Addition of autoinhibited UblR0RBR does not significantly enhance Miro1 ubiquitination (Fig 4c, Supp Fig 4b). However, addition of equimolar amounts of active UblR0RBR complexed with pUb rescues Miro1 ubiquitination to a greater extent than having the UblR0RBR.pUb complex alone (Fig 4c). These data suggest that the activity of inactive Parkin molecules can be stimulated by the presence of activated Parkin molecules. Taken together, these data demonstrate that Parkin molecules can function together to ligate ubiquitin.

Discussion

Previous extensive characterisation of Parkin has shown that Parkin exists in an autoinhibited state, mediated through multiple domain-domain interactions, including the UBL-RING1 interface, the REP blocking the proposed E2 binding site, and the proposed occlusion of the catalytic cysteine, Cys431, by the RING0 domain

330 [16,22-26]. All these inhibitory mechanisms are relieved by the activation of Parkin by
331 pUb [27,28,30]. pUb and the phosphorylated UBL domain are unable to simultaneously
332 bind to R0RBR Parkin in solution, *in trans*, suggesting an allosteric regulation of
333 Parkin by pUb binding [23,24,42,46]. In addition, previous studies have led to predictions
334 of large conformational changes in Parkin upon activation. Interestingly, a
335 computational analysis of Parkin suggest that phosphorylation of the UBL domain
336 initiates a large change, mediated by the 65 amino acid linker between the UBL
337 domain and RING0 (residues 77-140) [47]. An important caveat of our current
338 understanding of the mechanism of Parkin activity is that structures are either of
339 fragments of Parkin (R0RBR) [16,25,26], or all domains but lacking the UBL-RING0
340 linker [23,24]. However, in a low resolution structure of full length rat Parkin, the linker
341 is present in the protein, but is completely disordered in the crystal and can't be
342 modelled [25]. The UBL domain and R0RBR domains remain as they are in the absence
343 of the linker [23,24]. Interestingly, while the linker length, although not the composition,
344 is conserved down to *Drosophila* [23,24], Parkin from nematodes does not have a long
345 linker between the UBL and RING0 domains, therefore the functional importance of
346 this linker is still unclear. In this study, we present a modified model for Parkin
347 regulation, based on the first structures of an RBR ligase in the activated state,
348 complete with regulatory domains. Our structures reveal that in contrast to the large
349 conformational changes that have been predicted for Parkin function, activation of
350 Parkin results in local rearrangements of Parkin domains to reveal ubiquitin binding
351 sites. These ubiquitin binding sites recruit molecules of ubiquitin, or ubiquitin carried
352 by an E2, to bridge Parkin molecules and allow the utilisation of catalytic domains
353 from neighbouring molecules. In this model, the UBL-IBR interaction (Fig 5a) is
354 perturbed by UBL phosphorylation or pUb binding, displacing the IBR from the UBL

355 domain (Fig 5b/c). This IBR displacement opens a ubiquitin binding pocket on the
356 helix (H3)-IBR surface. A (donor) ubiquitin on loaded E2 occupies this new pocket
357 while E2 occupies the proposed sites on RING1, and the RING2(Rcat) of the
358 neighbouring molecule of Parkin (Fig 5d).

359 Based on current data, Parkin is unique in the RBR family in that it has a
360 distinct structural arrangement of RING1-IBR-RING2(Rcat) domains, where
361 RING2(Rcat) and RING1 are in juxtaposition. In contrast, in HOIP and HHARI
362 RING2(Rcat) and RING1 are separated by IBR (Supp Fig 5a) [37,44]. Although RBRs
363 share a conserved catalytic RING1-IBR-RING2(Rcat) module, they are usually
364 autoinhibited and activated via distinct mechanisms. pUb binding or UBL
365 phosphorylation releases Parkin autoinhibition [27-32], HOIP autoinhibition is released
366 by UBA mediated interactions with LUBAC constituents HOIL-1L or SHARPIN
367 [22,29,30,33,36,38,51] and HHARI autoinhibition is released by NEDD8 binding at the UBA
368 [38]. In the structure of full-length HHARI, the proposed NEDD8 binding pocket (Supp
369 Fig 5b) corresponds to the pocket is occupied by pUb or allosteric ubiquitin (Ub_{allo}) in
370 active Parkin or HOIP, respectively. This suggests that NEDD8 binding to HHARI
371 would have a similar effect as pUb or Ub_{allo} binding has on Parkin and HOIP. Inactive
372 HHARI and Parkin have a compact H3-IBR region (Supp Fig 5c). Active Parkin and
373 HOIP structures enable pUb or Ub_{allo} binding on one side of the H3-IBR region which
374 in the case of Parkin is occluded when inactive, and allows donor ubiquitin binding on
375 the opposite side of the H3-IBR (Supp Fig 5d). Therefore, we speculate that blocking
376 the donor ubiquitin binding site on one side of the H3-IBR, relieved upon pUb or
377 Ub_{allo} binding on the opposite side via opening of the H3-IBR to allow donor
378 ubiquitin binding, could be a common mechanism of regulation in RBR ligases.

The structure of HOIP-RBR in complex with loaded E2 also suggests that the RING1 and RING2(Rcat) of the same molecule cannot crosstalk as they are not close enough to allow catalysis of thioester formation, mediated by the catalytic cysteines of E2 and RING2(Rcat) (Supp Fig 5e). In the active state of HOIP-RBR the processive unit is formed by the RING2(Rcat) of molecule 1, and the RING1-IBR of a second molecule, where E2 interacts with the RING2(Rcat) of molecule 1 and RING1 of molecule 2 whereas the donor ubiquitin interacts with the RING2(Rcat) of molecule1 and the H3-IBR of molecule 2 (Supp Fig 5e). In contrast, in Parkin the processive unit is formed by RING1-RING2(Rcat) of molecule 1, and the IBR of molecule 2 (Fig 4d). This difference in the arrangement of domains between Parkin and HOIP, in the active state, is consistent with the differences in RING1-IBR-RING2(Rcat) structural organisation in three dimensions (Supp Fig 5a). Interestingly, inter/intra-molecular pairing of RING1-RING2(Rcat)-IBR domains of RBRs with E2 and donor ubiquitin explains the previous observations that Parkin and other RBRs favour the extended 'open' conformation of loaded E2 [44,45]. Furthermore, a role for Parkin oligomerisation or self-association has previously been reported [15], along with reports of Parkin having ubiquitin-binding activity [19,22]. Our structures of active Parkin support the idea that PINK1 induces structural changes in Parkin that stimulate ubiquitin binding. In the context of the mitochondrial membrane environment, where Parkin functions in mitophagy [52]), high local concentrations of Parkin, recruited by PINK1-catalysed phosphorylation of ubiquitin, could result in the feed-forward amplification of Parkin-mediated ubiquitination observed at the mitochondria [52,53]. Furthermore, it has been reported that Parkin functions with the linear chain assembly complex, LUBAC, comprising two RBR proteins in HOIP and HOIL-1L [54]. The structures reported here open up the possibility of cooperation between RBR modules,

404 and therefore we speculate that there is a possibility that RBR ligases can function in
405 concert.
406 Within the RBR module, it has long been predicted that RING1 recruits the E2
407 [55], recently formally demonstrated for HHARI and HOIP [44,45]; and that the
408 RING2(Rcat) domain, harbouring the catalytic cysteine, is the catalytic intermediate
409 domain [18]. However, a functional role for the IBR domain has been less clear. Our
410 observation that covalent modification in the IBR enhances Parkin activity, and that
411 deletion of IBR or mutations in IBR leads to loss of Parkin activity, coupled with a
412 recent report of increased Parkin activity after ISG15ylation on K349 and K363 of the
413 IBR [48], suggest a crucial role for the IBR in Parkin function. Our study suggests that
414 the role of the IBR, together with H3 (helix connecting RING1 and IBR), is to
415 mediate interactions with the inhibitory UBL domain in the inactive state, and the
416 donor ubiquitin in the active state, respectively. Furthermore, the IBR and
417 RING2(Rcat) of RBRs are structurally similar folds, each containing two β-hairpin
418 turns. Comparison of Parkin and HOIP structures in the active state reveals that the
419 IBR can interact with 2 ubiquitin molecules (pUb or $Ub_{allo,}$ and donor ubiquitin)
420 spanning across both β-hairpins (Supp Fig 5a). Similar to the IBR, the RING2(Rcat)
421 of HOIP also interacts with 2 ubiquitin molecules (donor and acceptor ubiquitin) [14,44]
422 mediated by both β-hairpins (Supp Fig 5f). Interestingly this observation furthers the
423 idea that the ubiquitination process is facilitated by the inherent ability of E1, E2 and
424 E3 proteins to interact with ubiquitin [56]. In our Parkin structures, only one ubiquitin
425 binding site is captured, predicted to be the donor ubiquitin binding site, while the
426 acceptor ubiquitin may occupy the opposite surface, in a manner similar to HOIP
427 (Supp Fig 5g); However, we cannot rule out that there may be subtle differences in

the acceptor ubiquitin or substrate recognition between RBRs that result in different type of modifications by different RBRs.

Taken together, our data suggest a common mechanism of regulation in RBRs. First, autoinhibition via blocking a donor ubiquitin binding pocket on H3-IBR. Second, release of autoinhibition by a UBL, be that phosphoubiquitin, NEDD8, ISG15, or ubiquitin itself, opening the H3-IBR binding site. Third, donor ubiquitin binding on the H3-IBR accompanied by a bridging of RBR molecules to facilitate access to the catalytic cysteine. Given the importance of Parkin function in mitophagy and PD, understanding the multiple regulatory modes required for function will provide a framework for the design of small molecules to modulate Parkin activity.

Acknowledgements

We thank L. Briere for her expertise and help in collecting and analyzing the sedimentation velocity data. This work was supported by the Cancer Research UK [grant number 17739]; the Medical Research Council [grant number MC_UU_12016/12]; and the EMBO Young Investigator Programme (HW). This work was supported by a grant from the Canadian Institutes of Health Research (MOP-14606) and the Canada Research Chairs Program (GSS).

Author contributions

AK designed and performed experiments, solved the crystal structures, analysed data and wrote the manuscript. VKC purified Miro1, made labelled ubiquitin and developed the labelled ubiquitin based assay, and performed the RING2(Rcat) loading experiments. TEC performed the NMR CSP experiments, KRB did the AUC

experiments. RT cloned several constructs. CJ, RS and AK purified various reagents for assays. GSS and HW designed the experiments, analysed data and wrote the manuscript.

Conflict of interest

I declare that the authors have no competing interests as defined by Springer Nature, or other interests that might be perceived to influence the results and/or discussion reported in this paper.

References

1. Bonifati, V. et al. Autosomal recessive early onset parkinsonism is linked to three loci: PARK2, PARK6, and PARK7. *Neurol Sci* **23 Suppl 2**, S59-60 (2002).
2. Martin, I., Dawson, V.L. & Dawson, T.M. Recent advances in the genetics of Parkinson's disease. *Annu Rev Genomics Hum Genet* **12**, 301-25 (2011).
3. Kitada, T. et al. Mutations in the parkin gene cause autosomal recessive juvenile parkinsonism. *Nature* **392**, 605-8 (1998).
4. Valente, E.M. et al. Hereditary early-onset Parkinson's disease caused by mutations in PINK1. *Science* **304**, 1158-60 (2004).
5. Chung, S.Y. et al. Parkin and PINK1 Patient iPSC-Derived Midbrain Dopamine Neurons Exhibit Mitochondrial Dysfunction and alpha-Synuclein Accumulation. *Stem Cell Reports* **7**, 664-677 (2016).
6. Exner, N., Lutz, A.K., Haass, C. & Winklhofer, K.F. Mitochondrial dysfunction in Parkinson's disease: molecular mechanisms and pathophysiological consequences. *EMBO J* **31**, 3038-62 (2012).
7. Narendra, D., Walker, J.E. & Youle, R. Mitochondrial quality control mediated by PINK1 and Parkin: links to parkinsonism. *Cold Spring Harb Perspect Biol* **4**(2012).
8. Walden, H. & Martinez-Torres, R.J. Regulation of Parkin E3 ubiquitin ligase activity. *Cell Mol Life Sci* **69**, 3053-67 (2012).
9. Dawson, T.M. & Dawson, V.L. The role of parkin in familial and sporadic Parkinson's disease. *Mov Disord* **25 Suppl 1**, S32-9 (2010).
10. Kahle, P.J. & Haass, C. How does parkin ligate ubiquitin to Parkinson's disease? *EMBO Rep* **5**, 681-5 (2004).
11. Lim, K.L., Dawson, V.L. & Dawson, T.M. Parkin-mediated lysine 63-linked polyubiquitination: a link to protein inclusions formation in Parkinson's and other conformational diseases? *Neurobiol Aging* **27**, 524-9 (2006).
12. Spratt, D.E., Walden, H. & Shaw, G.S. RBR E3 ubiquitin ligases: new structures, new insights, new questions. *Biochem J* **458**, 421-37 (2014).

13. Spratt, D.E. et al. A molecular explanation for the recessive nature of parkin-linked Parkinson's disease. *Nat Commun* **4**, 1983 (2013).
14. Stieglitz, B. et al. Structural basis for ligase-specific conjugation of linear ubiquitin chains by HOIP. *Nature* **503**, 422-6 (2013).
15. Lazarou, M. et al. PINK1 drives Parkin self-association and HECT-like E3 activity upstream of mitochondrial binding. *J Cell Biol* **200**, 163-72 (2013).
16. Riley, B.E. et al. Structure and function of Parkin E3 ubiquitin ligase reveals aspects of RING and HECT ligases. *Nat Commun* **4**, 1982 (2013).
17. Stieglitz, B., Morris-Davies, A.C., Koliopoulos, M.G., Christodoulou, E. & Rittinger, K. LUBAC synthesizes linear ubiquitin chains via a thioester intermediate. *EMBO Rep* **13**, 840-6 (2012).
18. Wenzel, D.M., Lissounov, A., Brzovic, P.S. & Klevit, R.E. UBCH7 reactivity profile reveals parkin and HHARI to be RING/HECT hybrids. *Nature* **474**, 105-8 (2011).
19. Zheng, X. & Hunter, T. Parkin mitochondrial translocation is achieved through a novel catalytic activity coupled mechanism. *Cell Res* **23**, 886-97 (2013).
20. Beasley, S.A., Hristova, V.A. & Shaw, G.S. Structure of the Parkin in-between-ring domain provides insights for E3-ligase dysfunction in autosomal recessive Parkinson's disease. *Proc Natl Acad Sci U S A* **104**, 3095-100 (2007).
21. Hristova, V.A., Beasley, S.A., Rylett, R.J. & Shaw, G.S. Identification of a novel Zn2+-binding domain in the autosomal recessive juvenile Parkinson-related E3 ligase parkin. *J Biol Chem* **284**, 14978-86 (2009).
22. Chaugule, V.K. et al. Autoregulation of Parkin activity through its ubiquitin-like domain. *EMBO J* **30**, 2853-67 (2011).
23. Kumar, A. et al. Disruption of the autoinhibited state primes the E3 ligase parkin for activation and catalysis. *EMBO J* **34**, 2506-21 (2015).
24. Sauve, V. et al. A Ubl/ubiquitin switch in the activation of Parkin. *EMBO J* (2015).
25. Trempe, J.F. et al. Structure of parkin reveals mechanisms for ubiquitin ligase activation. *Science* **340**, 1451-5 (2013).
26. Wauer, T. & Komander, D. Structure of the human Parkin ligase domain in an autoinhibited state. *EMBO J* **32**, 2099-112 (2013).
27. Kane, L.A. et al. PINK1 phosphorylates ubiquitin to activate Parkin E3 ubiquitin ligase activity. *J Cell Biol* **205**, 143-53 (2014).
28. Kazlauskaite, A. et al. Parkin is activated by PINK1-dependent phosphorylation of ubiquitin at Ser65. *Biochem J* **460**, 127-39 (2014).
29. Kondapalli, C. et al. PINK1 is activated by mitochondrial membrane potential depolarization and stimulates Parkin E3 ligase activity by phosphorylating Serine 65. *Open Biol* **2**, 120080 (2012).
30. Koyano, F. et al. Ubiquitin is phosphorylated by PINK1 to activate parkin. *Nature* **510**, 162-6 (2014).
31. Okatsu, K. et al. PINK1 autophosphorylation upon membrane potential dissipation is essential for Parkin recruitment to damaged mitochondria. *Nat Commun* **3**, 1016 (2012).
32. Shiba-Fukushima, K. et al. PINK1-mediated phosphorylation of the Parkin ubiquitin-like domain primes mitochondrial translocation of Parkin and regulates mitophagy. *Sci Rep* **2**, 1002 (2012).

33. Kirisako, T. et al. A ubiquitin ligase complex assembles linear polyubiquitin chains. *EMBO J* **25**, 4877-87 (2006).
34. Moynihan, T.P. et al. The ubiquitin-conjugating enzymes UbcH7 and UbcH8 interact with RING finger/IBR motif-containing domains of HHARI and H7-AP1. *J Biol Chem* **274**, 30963-8 (1999).
35. Smit, J.J. et al. The E3 ligase HOIP specifies linear ubiquitin chain assembly through its RING-IBR-RING domain and the unique LDD extension. *EMBO J* **31**, 3833-44 (2012).
36. Tokunaga, F. et al. SHARPIN is a component of the NF-kappaB-activating linear ubiquitin chain assembly complex. *Nature* **471**, 633-6 (2011).
37. Duda, D.M. et al. Structure of HHARI, a RING-IBR-RING ubiquitin ligase: autoinhibition of an Ariadne-family E3 and insights into ligation mechanism. *Structure* **21**, 1030-41 (2013).
38. Kelsall, I.R. et al. TRIAD1 and HHARI bind to and are activated by distinct neddylated Cullin-RING ligase complexes. *EMBO J* **32**, 2848-60 (2013).
39. Scott, D.C. et al. Two Distinct Types of E3 Ligases Work in Unison to Regulate Substrate Ubiquitylation. *Cell* **166**, 1198-1214 e24 (2016).
40. Caulfield, T.R., Fiesel, F.C. & Springer, W. Activation of the E3 ubiquitin ligase Parkin. *Biochem Soc Trans* **43**, 269-74 (2015).
41. Ham, S.J. et al. Interaction between RING1 (R1) and the Ubiquitin-like (UBL) Domains Is Critical for the Regulation of Parkin Activity. *J Biol Chem* **291**, 1803-16 (2016).
42. Kazlauskaite, A. et al. Binding to serine 65-phosphorylated ubiquitin primes Parkin for optimal PINK1-dependent phosphorylation and activation. *EMBO Rep* **16**, 939-54 (2015).
43. Wauer, T., Simicek, M., Schubert, A. & Komander, D. Mechanism of phospho-ubiquitin-induced PARKIN activation. *Nature* **524**, 370-4 (2015).
44. Lechtenberg, B.C. et al. Structure of a HOIP/E2~ubiquitin complex reveals RBR E3 ligase mechanism and regulation. *Nature* **529**, 546-50 (2016).
45. Dove, K.K., Stieglitz, B., Duncan, E.D., Rittinger, K. & Klevit, R.E. Molecular insights into RBR E3 ligase ubiquitin transfer mechanisms. *EMBO Rep* **17**, 1221-35 (2016).
46. Aguirre, J.D., Dunkerley, K.M., Mercier, P. & Shaw, G.S. Structure of phosphorylated UBL domain and insights into PINK1-orchestrated parkin activation. *Proc Natl Acad Sci U S A* **114**, 298-303 (2017).
47. Caulfield, T.R. et al. Phosphorylation by PINK1 releases the UBL domain and initializes the conformational opening of the E3 ubiquitin ligase Parkin. *PLoS Comput Biol* **10**, e1003935 (2014).
48. Im, E., Yoo, L., Hyun, M., Shin, W.H. & Chung, K.C. Covalent ISG15 conjugation positively regulates the ubiquitin E3 ligase activity of parkin. *Open Biol* **6**(2016).
49. Ordureau, A. et al. Defining roles of PARKIN and ubiquitin phosphorylation by PINK1 in mitochondrial quality control using a ubiquitin replacement strategy. *Proc Natl Acad Sci U S A* **112**, 6637-42 (2015).
50. Wauer, T. et al. Ubiquitin Ser65 phosphorylation affects ubiquitin structure, chain assembly and hydrolysis. *EMBO J* **34**, 307-25 (2015).
51. Tokunaga, F. et al. Involvement of linear polyubiquitylation of NEMO in NF-kappaB activation. *Nat Cell Biol* **11**, 123-32 (2009).
52. Lazarou, M. et al. The ubiquitin kinase PINK1 recruits autophagy receptors to induce mitophagy. *Nature* **524**, 309-14 (2015).

53. Ordureau, A. et al. Quantitative proteomics reveal a feedforward mechanism for mitochondrial PARKIN translocation and ubiquitin chain synthesis. *Mol Cell* **56**, 360-75 (2014).
54. Muller-Rischart, A.K. et al. The E3 ligase parkin maintains mitochondrial integrity by increasing linear ubiquitination of NEMO. *Mol Cell* **49**, 908-21 (2013).
55. Ardley, H.C., Tan, N.G., Rose, S.A., Markham, A.F. & Robinson, P.A. Features of the parkin/ariadne-like ubiquitin ligase, HHARI, that regulate its interaction with the ubiquitin-conjugating enzyme, Ubch7. *J Biol Chem* **276**, 19640-7 (2001).
56. Wright, J.D., Mace, P.D. & Day, C.L. Noncovalent Ubiquitin Interactions Regulate the Catalytic Activity of Ubiquitin Writers. *Trends Biochem Sci* **41**, 924-937 (2016).

Figure Legends

Figure 1 Overall structure of Parkin-phosphoubiquitin complex in the activated state

a) Crystal structure of UBLR0RBR and pUb complex showing UBL, RING0 , RING1, IBR, REP, and RING2(Rcat) of Parkin, in complex with phosphoubiquitin (blue). The phosphate group of phosphoubiquitin is shown in stick representation.

b) Comparison of UBLR0RBR-pUb complex (coloured) with the apo structure of UBLR0RBR (grey) (PDB code 5C1Z [23]). UBLR0RBR superimposed on the UBLR0RBR-pUb complex structure shows conformational changes between the IBR and the UBL domain, and the void formed (marked with arrow), helix 1 (H1) and helix 3 (H3) of RING1 are marked. UBL (green) remains associated with H1 of RING1 (cyan) in both apo and complex structures.

c) Isothermal Titration Calorimetry assays showing UBL interaction with ΔUBL Parkin (left panel), and that deletion of IBR in ΔUBL Parkin leads to loss of UBL and Parkin interaction (right panel).

d) Deletion of the IBR in ΔUBL Parkin leads to loss of E3 ligase activity of Parkin in ubiquitin chain formation, Parkin autoubiquitination, and Miro1

ubiquitination. FL (autoinhibited) or ΔUBL (active) Parkin comparison is shown with ΔUBL-ΔIBR Parkin, or ΔUBL-ΔIBR with a 10-residue linker in the presence or absence of pUb. Uncropped gel images are shown in Supplementary Data Set 1.

Figure 2 Identification of potential ubiquitin binding regions important for Parkin function.

a) Model of ubiquitin (grey surface) binding to Parkin, based on crystallographic packing of a second Parkin molecule (shown in Supp Fig 2b). The boundary of one UBLR0RBR-pUb complex (domains coloured as in Figure 1) is represented by a dashed line.

b) The UBL (green) and forms ubiquitin binding region 1 (UBR1) (left panel). For clarity, UBL (green), modelled ubiquitin (grey), RING1 helices H1, H3 (cyan), IBR (brown) are schematically represented below, with molecule 1 boundary of Parkin marked with a dashed line, and UBR1 marked as a shaded box. The activity of UBR1 mutants was monitored by fluorescently-labelled ubiquitin incorporation into ubiquitin chains and Parkin autoubiquitination, and Miro1 ubiquitination (right panel). Coomassie-stained gel is shown as loading control. In this and in all subsequent ubiquitination assays, a non-specific, ATP-independent band is indicated (*).

c) H3 of RING1 (cyan) and IBR (brown) make 2 important interfaces with ubiquitin (grey) (left upper panel), shown as UBR2 (purple box) and UBR3 (red box), respectively (left lower panel). Mutations in UBR2 and UBR3 of Parkin lead to loss of E3 ligase activity of Parkin in ubiquitin chain formation, Parkin

autoubiquitination, and Miro1 ubiquitination (right panel). Assay conditions are as in panel b.

d) Chemical shift perturbation map obtained from NMR titration experiments where $^{2}H,^{14}N$-labelled Ub was titrated into a solution of $^{2}H,^{12}C,^{15}N$-labelled R0RBR Parkin in complex with ^{2}H-labelled pUb, and followed by $^{1}H,^{15}N$ TROSY experiments. Residues that experienced chemical shift changes greater than 1 standard deviation above the average shift in the absence of Ub are indicated in yellow.

Figure 3 Parkin activation promotes donor ubiquitin (Ub_{don}) binding at H3-IBR interface

a) Nature of interactions (red sphere: electrostatic, black sphere: hydrophobic) between pUb (blue)/UB (grey) and H3 (cyan)/IBR (brown) of Parkin are shown schematically (left panel). Residues on H3 (cyan)-IBR (brown) of Parkin interacting with pUb (blue) and Ub (grey surface) (modelled by superposition on UBL of molecule 2 in the UBLR0RBR-pUb complex structure) are shown as sticks (middle panel). Helix-connecting-RING1-IBR and IBR of HOIP interaction with activator ubiquitin (Ub) and donor ubiquitin (Ub_{don}) (pdb code 5EDV [44]).

b) Isothermal Titration Calorimetry assays showing Glu321Ala mutation does not affect Parkin interaction with UbcH7 (upper panel), but does reduce Parkin interaction with the UbcH7~Ub iso-peptide (lower panel). ITC measurements were performed using phosphorylated Parkin in the presence of pUb.

c) Parkin can be activated by UbcH7C86K~pUb conjugate similarly to pUb. Ubiquitination assay was performed with 1μM of ParkinS65A. Parkin was activated with 1μM of UbS65A/pUb/UbcH7C86K~Ub/UbcH7C86K/

672 UbcH7C86K~pUb (Left panel), coomassie-stained gel is shown as loading control
673 (lower panel). A model depicting distinct ubiquitin (UbcH7~Ub or pUb/
674 UbcH7C86K~pUB) binding regions on Parkin is shown in the right panel.
675
676 **Figure 4 Parkin molecules cooperate to facilitate ubiquitin transfer**
677 **a**) Model of crystal packing between molecules of Parkin. The modelled donor
678 ubiquitin (grey surface) sits above the catalytic cysteine (C431) of the
679 RING2(Rcat) (red) of a neighbouring Parkin molecule. For clarity, the rest of the
680 Parkin molecules are shown in slate, except for the UBL domain (green), and IBR
681 (brown). The predicted E2 binding region on each molecule is shown.
682 **b**) Mutation of UBR2 and phosphoubiquitin patches of Parkin leads to defects in
683 formation of a RING2(Rcat)-Ub ester intermediate, monitored using fluorescently-
684 labelled ubiquitin (left top). Sodium hydroxide sensitivity confirms the
685 RING2(Rcat)-ubiquitin ester bond (left bottom). Coomassie-stained gels are shown
686 as total Parkin levels. Integrated intensities of Parkin-Ub ester levels from three
687 independent experiments were plotted as mean ± SEM (right). Statistical
688 significance was determined by one-way analysis of variance with Bonferroni's
689 multiple-comparison test. (n = 3, ****P < 0.0001).
690 **c**) Activated UblR0RBR complexed with phosphoubiquitin can stimulate the
691 activity of inactive Parkin. The activity of phosphoParkin mutated in the ubiquitin
692 donor binding site (E321A) is enhanced by the addition of UblR0RBR Parkin
693 covalently complexed with phosphoubiquitin. Addition of UblR0RBR Parkin
694 alone does not enhance the activity of pParkinE321A. Ubiquitination of Miro1 is
695 monitored using fluorescently-labelled ubiquitin (left top). Coomassie stained gel
696 shows total Miro1 levels (left bottom). Integrated intensities of Miro1-Ub levels

from three independent experiments were plotted as mean ± SEM (right). Statistical significance was determined by one-way analysis of variance with Bonferroni's multiple-comparison test. (n = 3, ****P < 0.0001, **P < 0.01)

Figure 5 Model of Parkin regulation

a) Parkin is autoinhibited by UBL blocking IBR (brown) and H3 (red) of RING1 (cyan).

b) Phosphorylation (marked with red asterisk) of UBL/pUb binding creates a pocket at H3-IBR and UBL interface, leading to activated Parkin.

c) Activated Parkin shows small rearrangements triggered by the straightening of the H3-IBR helix. Loaded E2 (E2~Ub) is recognised at this new interface, E2 occupying interface with REP and RING1 of activated Parkin, Ub_{don} (grey) sitting on the interface of IBR (brown box) and H3 (red helix) of RING1 of neighbouring molecule of Parkin (marked with a dashed line).

Table 1

Table 1 Data collection and refinement statistics (molecular replacement)

	UBLR0RBR+pUb (5N2W)	S65DUBLR0RBR+pUb (5N38)
Data collection		
Space group	P63 2 2	P63 2 2
Cell dimensions		
a, *b*, *c* (Å)	147.3 147.3 87.5	146.5 146.5 88.4
α, β, γ (°)	90 90 120	90 90 120
Resolution (Å)	56.34-2.68 (2.81-2.68)[a]	72.56-2.60 (2.76-2.60)[a]
R_{merge}	10.7 (71.9)	8.2 (48.4)
$I/\sigma(I)$	8.9 (1.9)	9.1 (2.2)
$CC_{1/2}$	99.4 (66.8)	99.5 (64.0)
Completeness (%)	93.6 (93.7)	96.4 (88.4)
Redundancy	4.6 (4.2)	3.5 (3.2)
Refinement		
Resolution (Å)	56.34 (2.68)	72.56 (2.60)
No. reflections	15007	16984
R_{work} / R_{free}	19.93/24.17	18.16/22.86

No. atoms		
Protein	3619	3565
Ligand/ion	23[a]	17[b]
Water	29	46
B factors		
Protein	60.2	55.9
Ligand/ion	84.4	79.1
Water	53.4	37.8
R.m.s. deviations		
Bond lengths (Å)	0.01	0.01
Bond angles (°)	1.14	1.17

715 Single crystals were used for structure determination.
716 [a]8 Zinc ions, 1 Chloride ion, 10 trimethyloxide atoms, 4 aminopropane atoms
717 [b]8 Zinc ions, 1 Chloride ion, 4 polyethylene glycol atoms, 4 aminopropane atoms

Online Methods

Protein expression and purification

UBLR0RBRGln347Cys (resi 1-83, 144-465) and S65DUBLR0RBRgln347Cys (resi 1-83, 144-465) were expressed as His-Smt-3 fusion. FL, various mutants and truncated constructs of Parkin were expressed as His-SUMO fusion. Constructs were expressed in in BL21 (DE3) *E. coli* cells and purified as previously described (21,22). Parkin or ubiquitin were phosphorylated using *Pediculus humanus* PINK1 (126-C) or *Tribolium castaneum* PINK1 (TcPINK1), expressed and purified as previously described [23,57]. Miro1 (181-592) and fluorescently labelled ubiquitin (Ub^{IR800}) were prepared as previously described [23].

Preparation of phospho-Ubiquitin-3BR probe

Ubiquitin was expressed as ubiquitin 1-75-Mxe-intein/chitin binding domain using pTXB-1 vector ((DU49003)) in BL21 *E. coli* cells. Cells were induced at 0.5 OD_{600} with 300μM IPTG (Isopropyl β-D-1-thiogalactopyranoside) and incubated at 20°C overnight. Cells were lysed in lysis buffer (20mM Na_2HPO_4 pH7.2, 200mM NaCl and 0.1mM EDTA). Clear lysate was incubated with Chitin resin, after washing with 2-column volume of lysis buffer protein was eluted in 20mM Na_2HPO_4 pH6.0, 200mM NaCl and 0.1mM EDTA and 0.1mM MESNA (Sodium 2-mercaptoethanesulfonate). Eluted material was reacted with 3-Bromo-propyl amine hydrobromide (SIGMA) as described before [58,59]. After reaction, protein was purified on size-exclusion column pre-equilibrated with PBS. Fractions containing ubiquitin were collected and phosphorylated using *Pediculus humanus* GST-PINK1, and further purified by size-exclusion chromatography. M1-$(UbS65A)_3$-pUb-3BR was prepared similarly by expressing M1 linked linear tetra-ubiquitin, in the same vector, with distal ubiquitins' Ser65 mutated to Ala.

744

745 **Preparation of UBLR0RBR347Cys~pUb/S65DUBLR0RBR347Cys~pUb**

746 We first mutated UBLR0RBR Parkin to contain a cysteine residue at position 347.
747 The corresponding residue in *Pediculus humanus* Parkin is a cysteine, and this
748 enabled R0RBR Parkin to react with the phosphoubiquitin-3BR probe, as described
749 previously [43]. UBLR0RBRGln347Cys/S65DUBLR0RBRGln347Cys was reacted
750 with 3 fold molar excess of pUb-3BR probe at room temperature for 2hrs. Complex
751 was purified by size-exclusion chromatography in 20mM Tris pH7.5, 75mM NaCl
752 and 250μM TCEP buffer. UBLR0RBR347Cys~pUb-(M1-UbS65A)$_3$ was prepared
753 using the same method.

754

755 **Crystallisation and Structure determination**

756 UBLR0RBRGln347Cys/S65DUBLR0RBRGln347Cys~pUb were crystallised at 4°C
757 in sitting drop plates by mixing 1:1 of protein (7mg/ml) and mother liquor (100mM
758 Tris pH 8.5, 200mM TMAO, PEG MME 2000). Crystals were flash frozen in liquid
759 nitrogen using 20% of PEG400 as cryo-protectant in the original mother liquor. Data
760 were collected at Diamond Light Source, wavelength 0.979Å. Data were solved by
761 molecular replacement program Phaser in CCP4 [60] by using UBL (1-76), RING0
762 (142-216), RING1 (229-328), IBR (329-377) and RING2(Rcat) (415-465) domains of
763 apo Parkin structure (5c1z) and pUb (4wzp) as ensembles. Solution obtained by
764 phaser was built and refined in iterative cycles by using coot [61] and autobuster [62],
765 respectively. Ramachandran values were calculated using Molprobity [63]. Both
766 structures have excellent geometry with ~95% of residues in the most favoured
767 regions. The structure coordinates and structure factors have been deposited in the
768 Protein Data Bank, with the accession codes 5N2W and 5N38.

769

770 **Size-exclusion chromatography**

771 Size-exclusion chromatography experiment was performed on analytical column
772 superdex-75, pre-equilibrated with 50mM HEPES pH 7.5, 200mM NaCl, 250μM of
773 TCEP. 10μM of Phospho-Parkin was incubated with 2 fold molar excess of pUb or
774 pUb and UbcH7~Ub for 1 hr prior to loading on column. UbcH7~Ub was prepared as
775 described previously [23].

776

777 **Isothermal titration calorimetry**

778 ITC experiments were performed using PEAQ-ITC (Malvern instruments), and data
779 were analysed using single-site binding model. 30μM of WT-Phospho-
780 Parkin/Phospho-ParkinGlu321Ala (premixed with 1.2 fold molar excess of pUb) were
781 titrated using 1.6mM or 1.48mM of UbcH7 in the syringe, respectively. 21.4μM of
782 ΔUBL, 40μM of ΔUBL (Gln389Ala, Tyr291Ala, Arg392Ala) premixed with 1.2 fold
783 molar excess of pUb, and 19μM of ΔUBL-ΔIBR were titrated using 1.14mM, 750μM,
784 500μM of WT UBL domain in the syringe, respectively. UbcH7 and UBL titrations
785 were performed at 20°C in 50mM HEPES pH 7.5, 200mM NaCl, 250μM of TCEP
786 and PBS, 500μM of TCEP, respectively.

787

788 **Ubiquitination assay**

789 Ubiquitination reactions were performed at 30°C in 50mM Tris pH 7.5, 100mM
790 NaCl, 2.5mM $Mgcl_2$, 5% glycerol, 500μM TCEP. Ubiquitin chain extension reactions
791 contained 25nm of recombinant human E1, 500nM of UbcH7, 1μM E3 and 5mM of
792 ATP in 20 μl of final reaction volume. 0.5 μM of pUB/ WT-UB was used as an
793 allosteric activator in various reactions. Ubiquitination reaction was analysed using

3μM of fluorescently labelled ubiquitin (Ub^{IR800}). Ubiquitin labelling was performed using DyLight$^{TM\ 800}$ Maleimide as described before [23]. Miro1 ubiquitination was performed in the similar setup using 5μM of Miro1 (181-592) and 12.5nm of recombinant human E1, 250nM of UbcH7, 0.5μM E3 and 5mM of ATP in 20 μl of final reaction volume. For Figure 3d, UBS65A/WT-Ub/UbcH7C86K/UbcH7C86K~Ub were phosphorylated in separate reactions with GST tagged TcPINK1; UbcH7C86K~Ub with no PINK1 was used as control. Prior to addition to Ubiquitination reaction, PINK1 was depleted using GST resin. Miro1 ubiquitination was performed in the similar setup using 5μM of Miro1 (181-592) and 12.5nm of recombinant human E1, 250nM of UbcH7, 0.5μM (unless otherwise specified) E3 and 5mM of ATP in 20 μl of final reaction volume. All assays were repeated at least 3 times.

Parkin ubiquitin loading

Reactions monitoring RING2(Rcat)-ubiquitin ester formation were performed at 30°C for 90 min in 50mM Tris pH 7.5, 100mM NaCl, 5mM $MgCl_2$, 1mM TCEP and 0.5% polyethylene glycol 6000 reaction buffer. Reactions contained 50nm E1, 10μM UbcH7, 10μM Ub^{IR800}, 3μM E3 and 5mM ATP in final reaction volume of 10μl. Non-activatable pUb-6His (3μM) was used as an allosteric activator where indicated. Reactions were stopped using NuPAGE LDS Sample Buffer (Invitrogen) that contained reducing agents and boiled for 5min. To hydrolyse ester linkages the boiled samples were cooled and further treated with 0.4M NaOH for 20 min at 42°C. The samples were resolved by SDS-PAGE and analyzed by direct fluorescence monitoring using Li-COR Odyssey Infrared Imaging System. Integrated intensities of Parkin-Ub ester species from three independent experiments were obtained using

819 Image Studio (Odyssey) imaging software, plotted as mean ± standard error of mean
820 (SEM) and statistically analysed using GraphdPad Prism7.
821
822 **Chemical Shift Perturbations**
823 A complex of $^{2}H,^{12}C,^{15}N$-labelled R0RBR with ^{2}H-labelled pUb (prepared as above)
824 was purified to homogeneity using gel filtration chromatography in 25 mM HEPES,
825 100 mM NaCl, 0.5 mM TCEP at pH 7.0. Chemical shift perturbation experiments
826 were measured using $^{1}H,^{15}N$-TROSY spectra of 205 µM $^{2}H,^{12}C,^{15}N$-R0RBR/ ^{2}H-pUb
827 in the absence and presence of $^{2}H,^{14}N$-labelled Ub. These experiments were
828 quantified using the following weighted formula: $((0.2 \times \Delta\delta N^2) + \Delta\delta H^2)^{1/2}$ and
829 plotted as a function of residue. All NMR experiments were collected using a triple
830 resonance cryogenic probe on a Varian Inova 600 MHz NMR spectrometer at 25˚C.
831
832 **Accession codes**
833 The protein structure files reported in this manuscript are available from the Protein
834 Data Bank with accession codes 5N2W, and 5N38.
835
836 **Data availability statement**
837 All constructs are available on request from the MRC Protein Phosphorylation and
838 Ubiquitylation Unit reagents Web page (http://mrcppureagents.dundee.ac.uk). All
839 other data are available from corresponding author upon reasonable request.
840
841 **Methods-only references**
842 57. Woodroof, H.I. et al. Discovery of catalytically active orthologues of the
843 Parkinson's disease kinase PINK1: analysis of substrate specificity and impact
844 of mutations. *Open Biol* **1**, 110012 (2011).

58. Abdul Rehman, S.A. et al. MINDY-1 Is a Member of an Evolutionarily Conserved and Structurally Distinct New Family of Deubiquitinating Enzymes. *Mol Cell* **63**, 146-55 (2016).
59. Borodovsky, A. et al. Chemistry-based functional proteomics reveals novel members of the deubiquitinating enzyme family. *Chem Biol* **9**, 1149-59 (2002).
60. Collaborative Computational Project, N. The CCP4 suite: programs for protein crystallography. *Acta Crystallogr D Biol Crystallogr* **50**, 760-3 (1994).
61. Emsley, P. & Cowtan, K. Coot: model-building tools for molecular graphics. *Acta Crystallogr D Biol Crystallogr* **60**, 2126-32 (2004).
62. Bricogne, G. et al. BUSTER 2.11.2. Cambridge, UK: Global Phasing Ltd. (2011).
63. Chen, V.B. et al. MolProbity: all-atom structure validation for macromolecular crystallography. *Acta Crystallogr D Biol Crystallogr* **66**, 12-21 (2010).

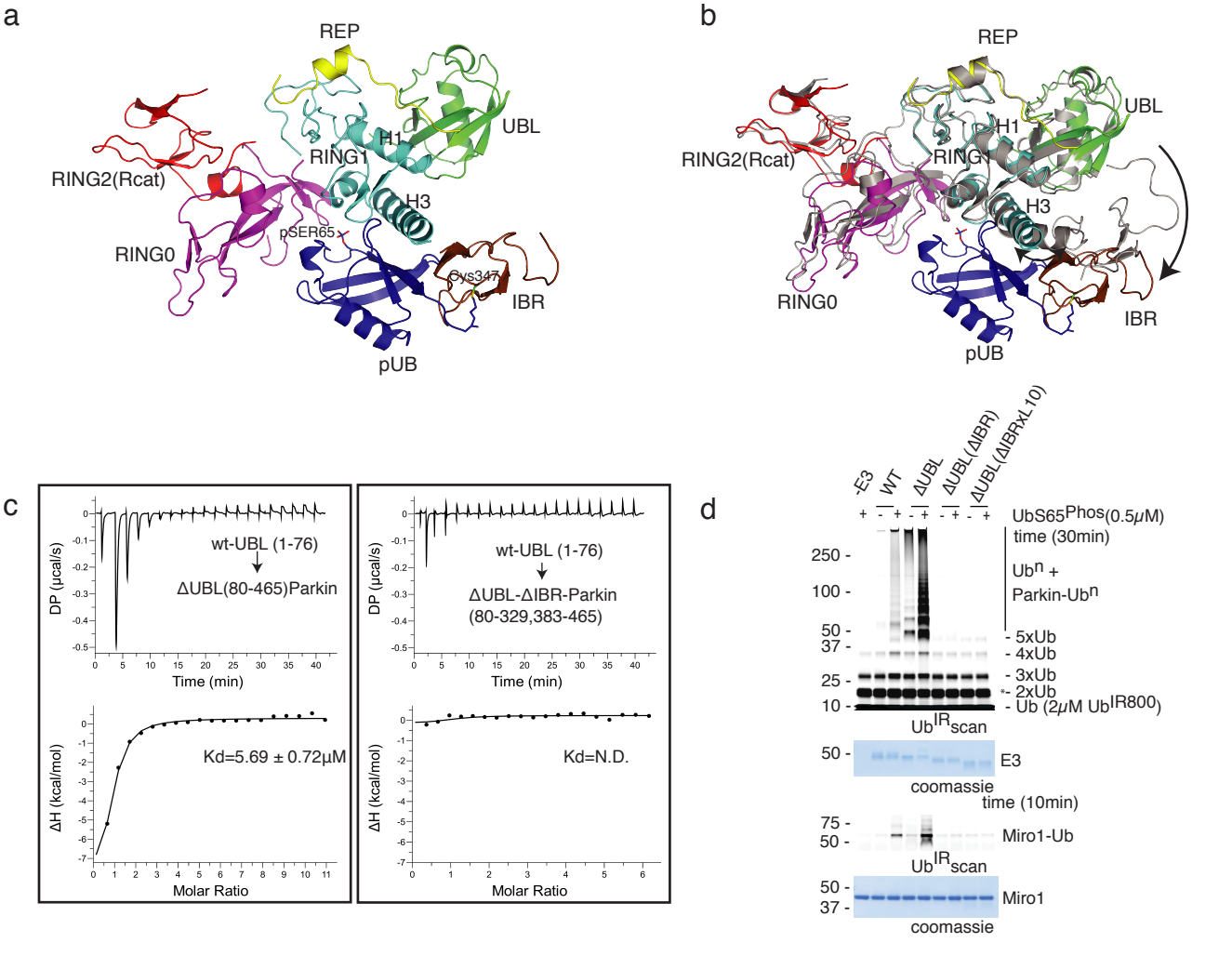
a
REP
UBL
H1
RING1
RING2(Rcat)
H3
pSER65
RING0
Cys347
IBR
pUB
b
REP
UBL
H1
RING1
RING2(Rcat)
H3
RING0
IBR
pUB
c
wt-UBL (1-76)
ΔUBL(80-465)Parkin
DP (μcal/s)
Time (min)
ΔH (kcal/mol)
Kd=5.69 ± 0.72μM
Molar Ratio
wt-UBL (1-76)
ΔUBL-ΔIBR-Parkin
(80-329,383-465)
DP (μcal/s)
Time (min)
ΔH (kcal/mol)
Kd=N.D.
Molar Ratio
d
-E3
WT
ΔUBL
ΔUBL(ΔIBR)
ΔUBL(ΔIBRxL10)
UbS65Phos(0.5μM)
time (30min)
Ubn +
Parkin-Ubn
250 -
100 -
50 -
37 -
25 -
10 -
- 5xUb
- 4xUb
- 3xUb
*- 2xUb
- Ub (2μM UbIR800)
UbIRscan
50 -
E3
coomassie
time (10min)
75 -
50 -
Miro1-Ub
UbIRscan
50 -
37 -
Miro1
coomassie

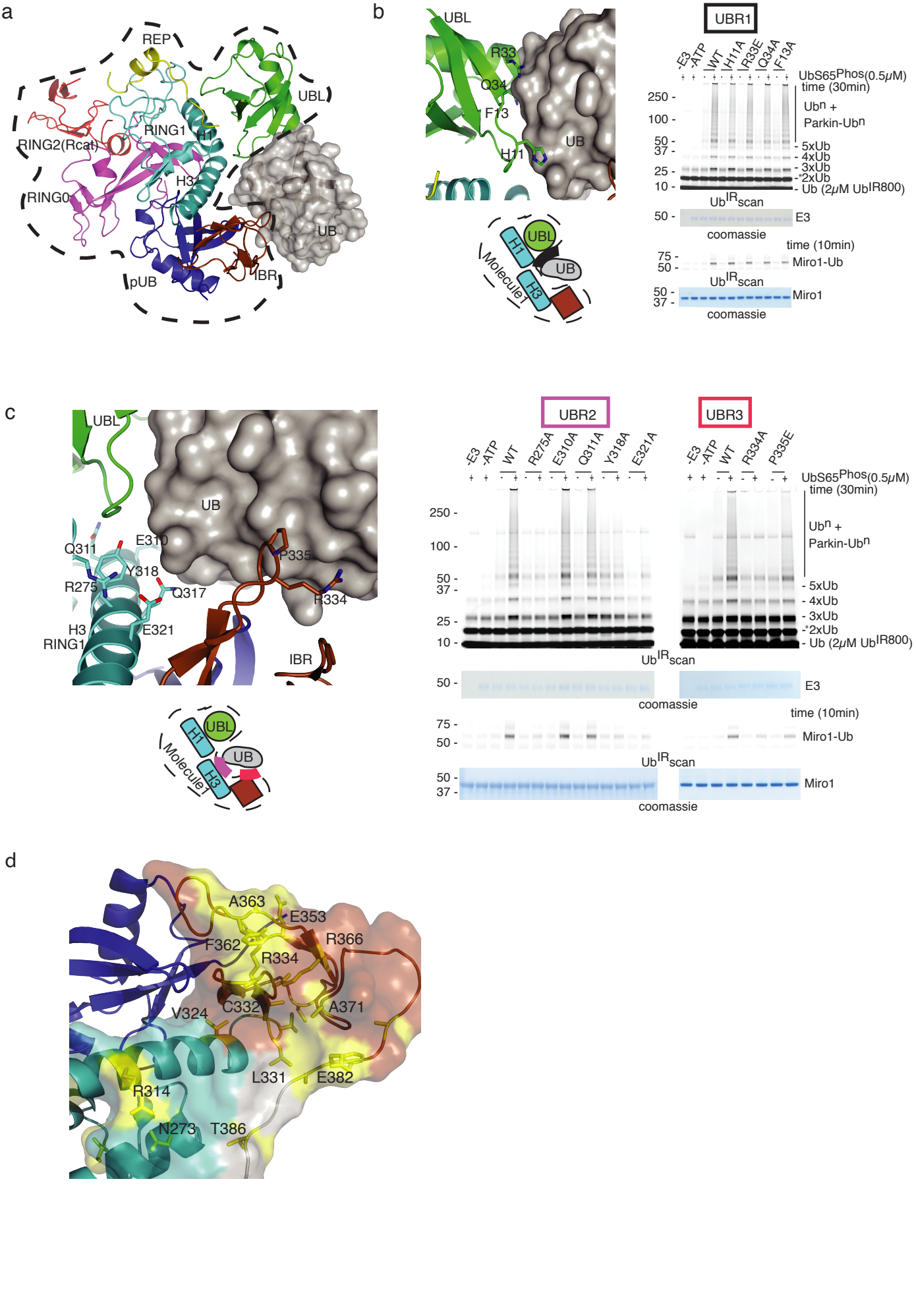
a
REP
UBL
RING1
H1
RING2(Rcat)
H3
RING0
UB
pUB
IBR
b
UBL
R33
Q34
F13
H11
UB
UBL
H1
UB
H3
Molecule1
UBR1
-E3
-ATP
WT
H11A
R33E
Q34A
F13A
UbS65Phos(0.5μM)
time (30min)
250 -
100 -
50 -
37 -
25 -
10 -
Ubn +
Parkin-Ubn
5xUb
4xUb
3xUb
*2xUb
Ub (2μM UbIR800)
UbIRscan
50 -
E3
coomassie
time (10min)
75 -
50 -
Miro1-Ub
UbIRscan
50 -
37 -
Miro1
coomassie
c
UBL
UB
Q311
E310
P335
Y318
R275
Q317
R334
H3
RING1
E321
IBR
UBL
H1
UB
H3
Molecule1
UBR2
UBR3
-E3
-ATP
WT
R275A
E310A
Q311A
Y318A
E321A
WT
R334A
P335E
UbS65Phos(0.5μM)
time (30min)
250 -
100 -
50 -
37 -
25 -
10 -
Ubn +
Parkin-Ubn
5xUb
4xUb
3xUb
*2xUb
Ub (2μM UbIR800)
UbIRscan
50 -
E3
coomassie
time (10min)
75 -
50 -
Miro1-Ub
UbIRscan
50 -
37 -
Miro1
coomassie
d
A363
E353
F362
R366
R334
C332
V324
A371
L331
E382
R314
N273
T386

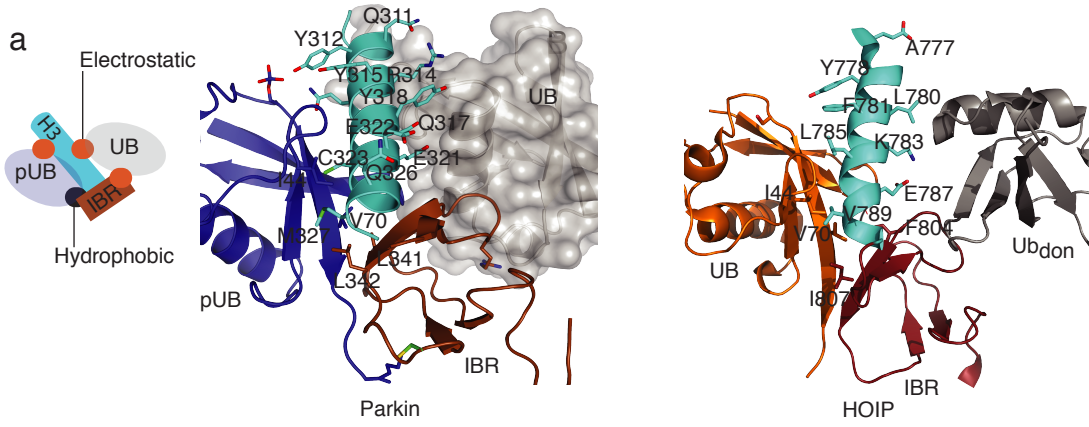
a
Electrostatic
H3
UB
pUB
IBR
Hydrophobic
Q311
Y312
Y315
R314
Y318
UB
E322
Q317
C323
E321
Q326
V70
M321
L341
L342
pUB
IBR
Parkin
A777
Y778
L780
F781
L785
K783
E787
L789
F804
Ubdon
UB
I807
IBR
HOIP

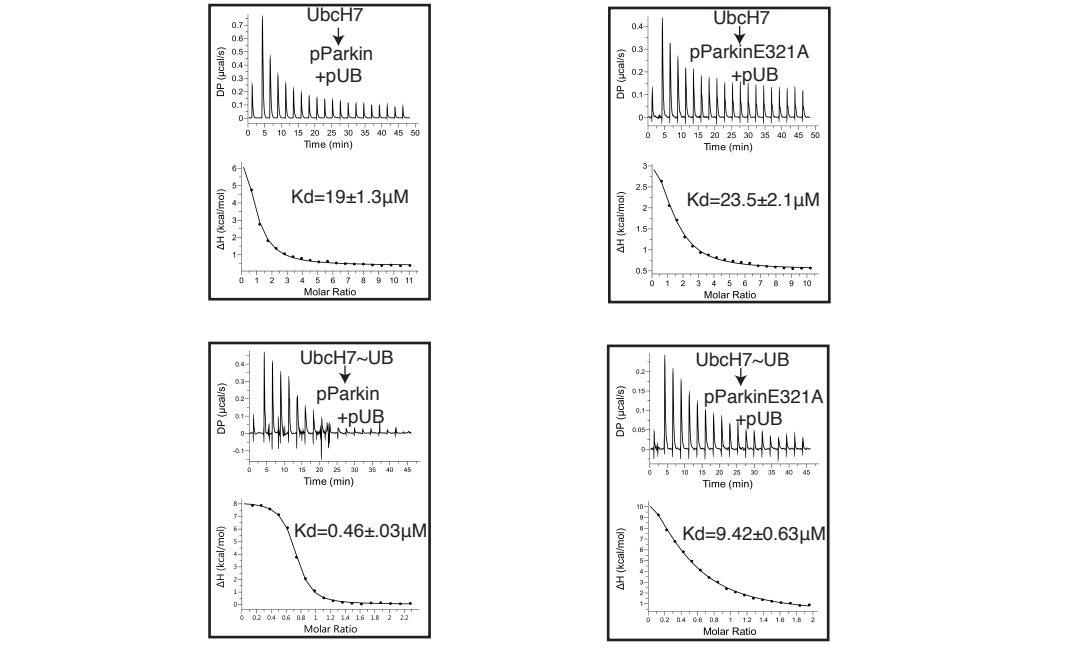
b
UbcH7
pParkin
+pUB
Kd=19±1.3μM
UbcH7
pParkinE321A
+pUB
Kd=23.5±2.1μM
UbcH7~UB
pParkin
+pUB
Kd=0.46±.03μM
UbcH7~UB
pParkinE321A
+pUB
Kd=9.42±0.63μM
DP (μcal/s)
Time (min)
ΔH (kcal/mol)
Molar Ratio

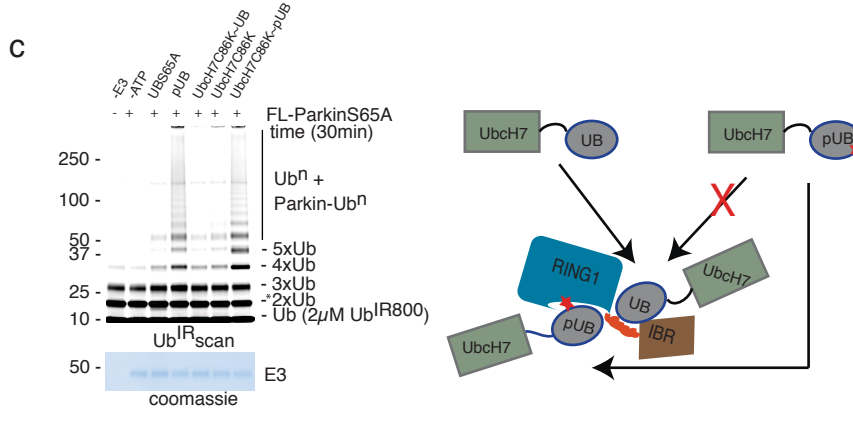
c
-E3
-ATP
UBS65A
pUB
UbcH7C86K-UB
UbcH7C86K
UbcH7C86K-pUB
FL-ParkinS65A
time (30min)
250 -
100 -
50 -
37 -
25 -
10 -
Ub^n +
Parkin-Ub^n
- 5xUb
- 4xUb
- 3xUb
- 2xUb
- Ub (2μM Ub^IR800)
Ub^IR scan
50 -
E3
coomassie
UbcH7
UB
UbcH7
pUB
RING1
UB
pUB
IBR
UbcH7
UbcH7

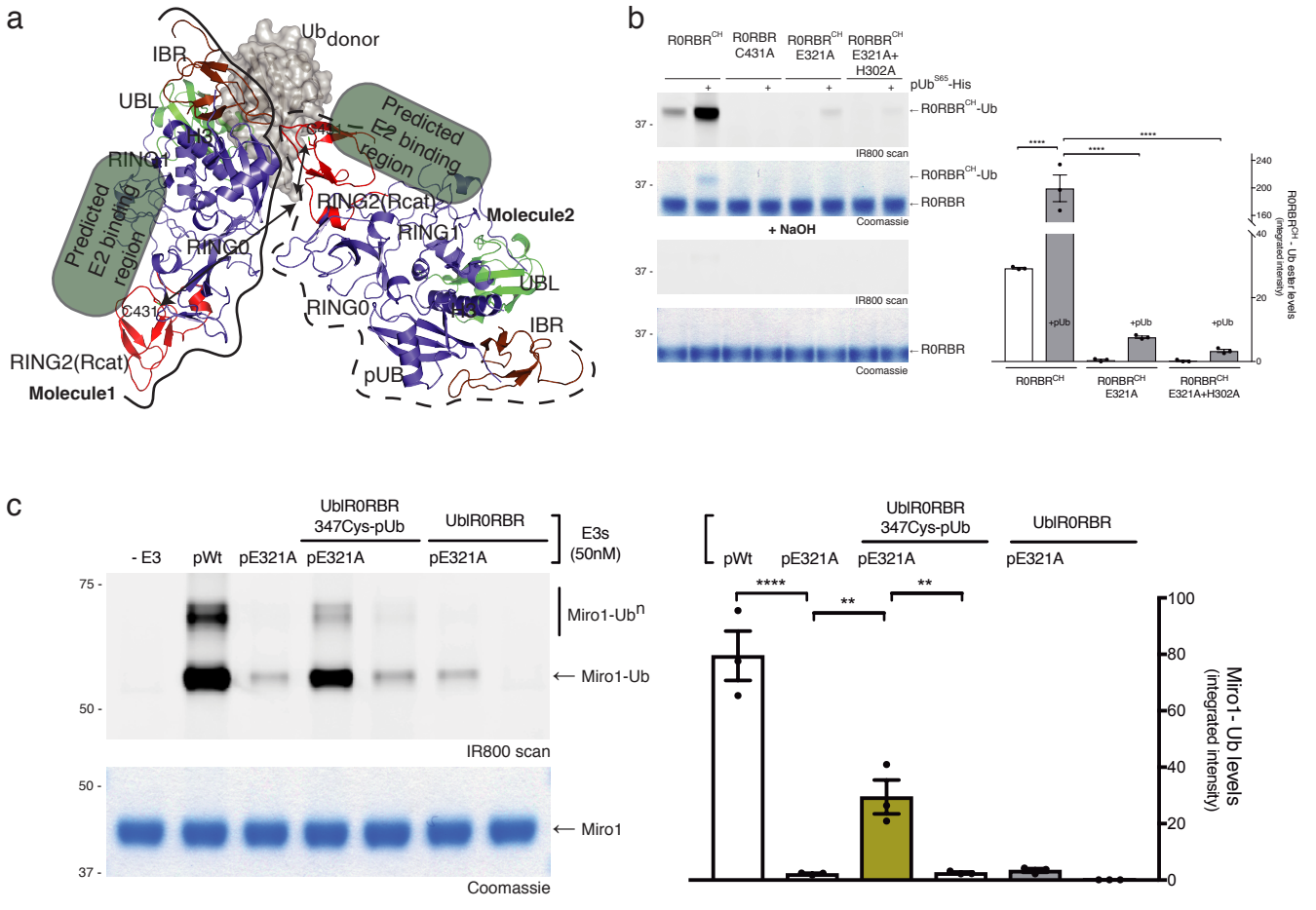
a
Ub donor
IBR
UBL
H302
RING1
Predicted E2 binding region
Predicted E2 binding region
RING2(Rcat)
Molecule2
RING1
RING0
UBL
C431
RING0
IBR
pUB
RING2(Rcat)
Molecule1
b
R0RBR^CH
R0RBR C431A
R0RBR^CH E321A
R0RBR^CH E321A+ H302A
pUb^S65-His
← R0RBR^CH-Ub
IR800 scan
← R0RBR^CH-Ub
← R0RBR
Coomassie
+ NaOH
IR800 scan
← R0RBR
Coomassie
R0RBR^CH - Ub ester levels (integrated intensity)
+pUb
R0RBR^CH
R0RBR^CH E321A
R0RBR^CH E321A+H302A
c
UblR0RBR 347Cys-pUb
UblR0RBR
E3s (50nM)
- E3
pWt
pE321A
pE321A
pE321A
Miro1-Ub^n
← Miro1-Ub
IR800 scan
← Miro1
Coomassie
Miro1-Ub levels (integrated intensity)

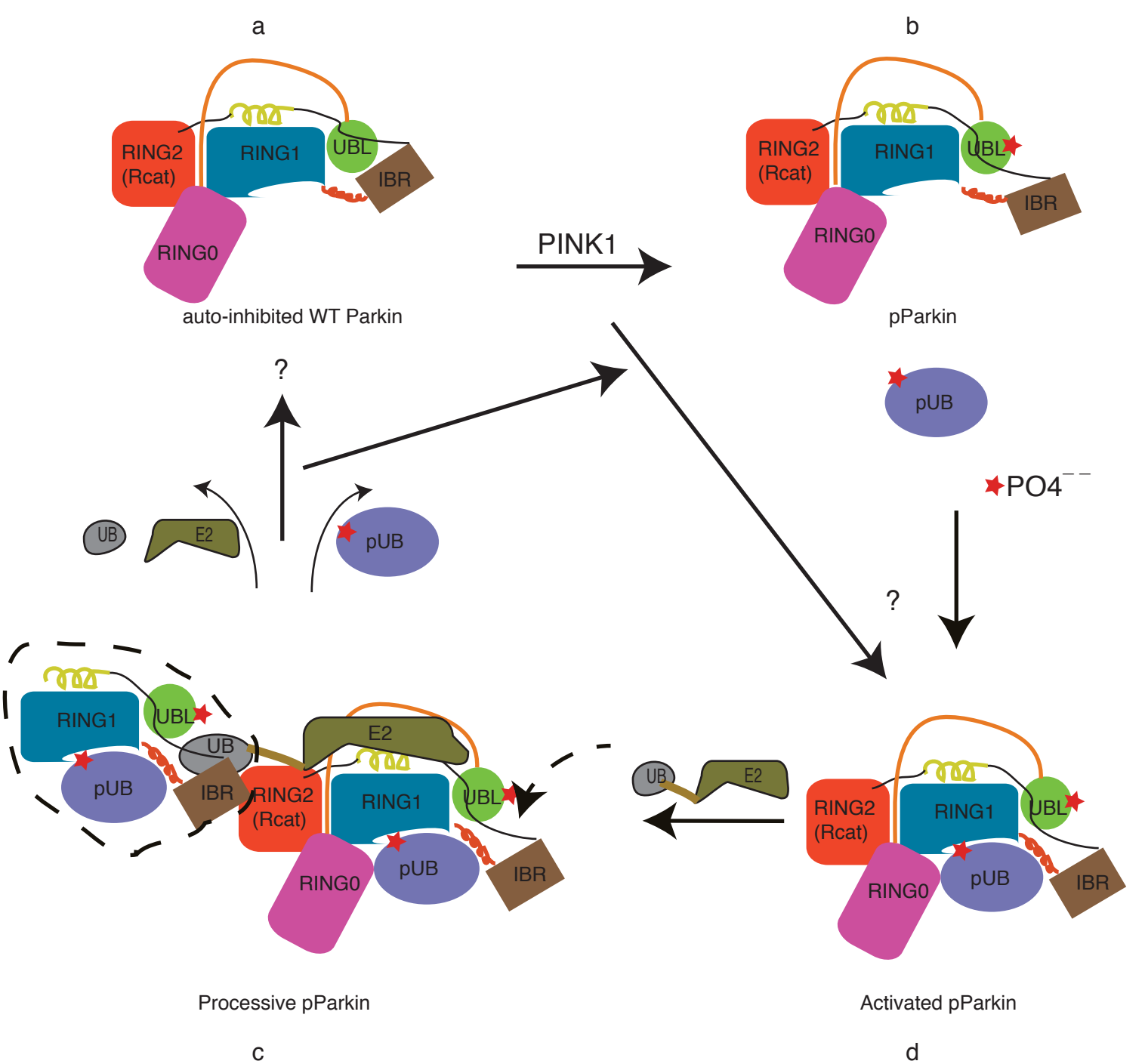
a
b
RING2
(Rcat)
RING1
UBL
IBR
RING0
PINK1
auto-inhibited WT Parkin
pParkin
?
pUB
PO4
UB
E2
?
RING1
UBL
UB
pUB
IBR
E2
RING2
(Rcat)
RING1
UBL
RING0
pUB
IBR
Processive pParkin
Activated pParkin
c
d

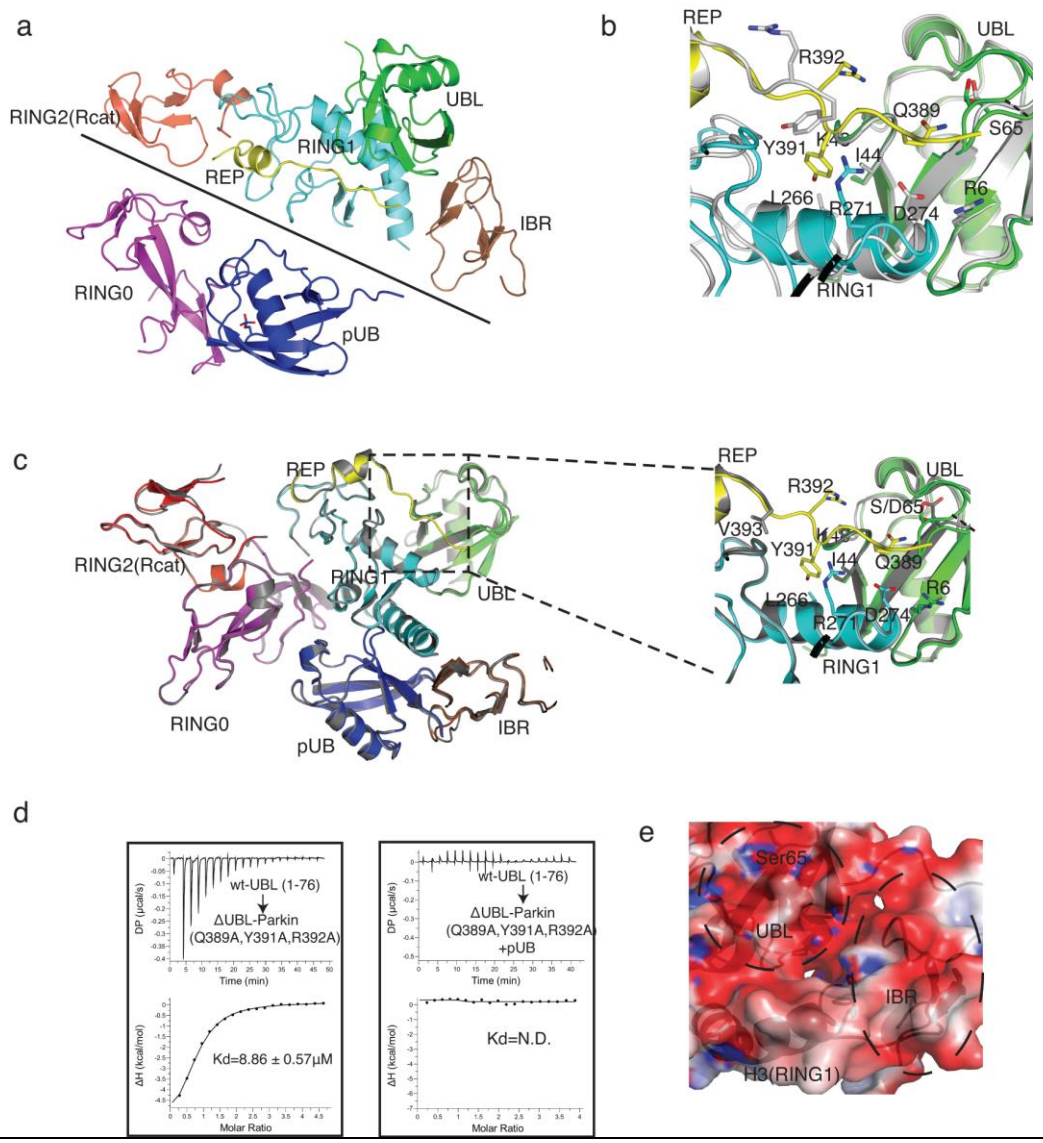

Supplementary Figure 1

UBL and RING1 interface remain associated in the complex structures of Parkin and pUb

a) Asymmetric Unit of crystal structure of UBLR0RBR and pUb complex showing UBL (green), RING1 (cyan), IBR (brown), REP (yellow), and RING2(Rcat) (red) of one molecule, RING0 (magenta) and pUb (blue) from another molecule (upper panel). The interface between the two molecules is marked with a solid line. The biological unit of active Parkin complexed with pUb is generated using domains from symmetry-related molecules of Parkin (Lower panel). The phosphate group of pUb is shown in stick representation. **b**) Superposition of UBLR0RBR-pUb complex structure, UBL (green), RING1 (cyan), REP (yellow), with apo structure of UBLR0RBR (grey) (pdb code: 5C1Z). Important residues at UBL-RING1 interface, and the tether connecting IBR and REP are shown as sticks. UBLR0RBR-pUb complex structure showing alternate conformations of flexible loop (62-65) movement is marked with dashed line, Ser65 is shown as stick. **c**) Superposition of UBLR0RBR-pUb complex structure coloured as in b, with the S65DUBLR0RBR-pUb complex structure (grey). Important residues in the tether and the UBL-IBR interface are shown as sticks in the close-up (right). **d)** Isothermal Titration Calorimetry assays showing UBL interaction with ΔUBL Parkin tether mutants (Q389A, Y391A, R392A) in the absence (left) and presence (right) of phosphoubiquitin. Tether mutants (Q389A, Y391A, R392A) in ΔUBL Parkin do not rescue the loss of UBL and Parkin association in the presence of pUb). **e)** Electrostatic charge surface of Parkin showing negatively charged region at the interface of UBL and IBR, Ser65 on UBL is shown as stick. The electrostatic potential is calculated with the program APBS (Baker NA, Sept D, Joseph S, Holst MJ, McCammon JA. Electrostatics of nanosystems: application to microtubules and the ribosome. *Proc Natl Acad Sci USA.* 2001 98(18):10037-41.). The surface is coloured with a blue to red gradient from +2.5 to −2.5 K_bT/e.

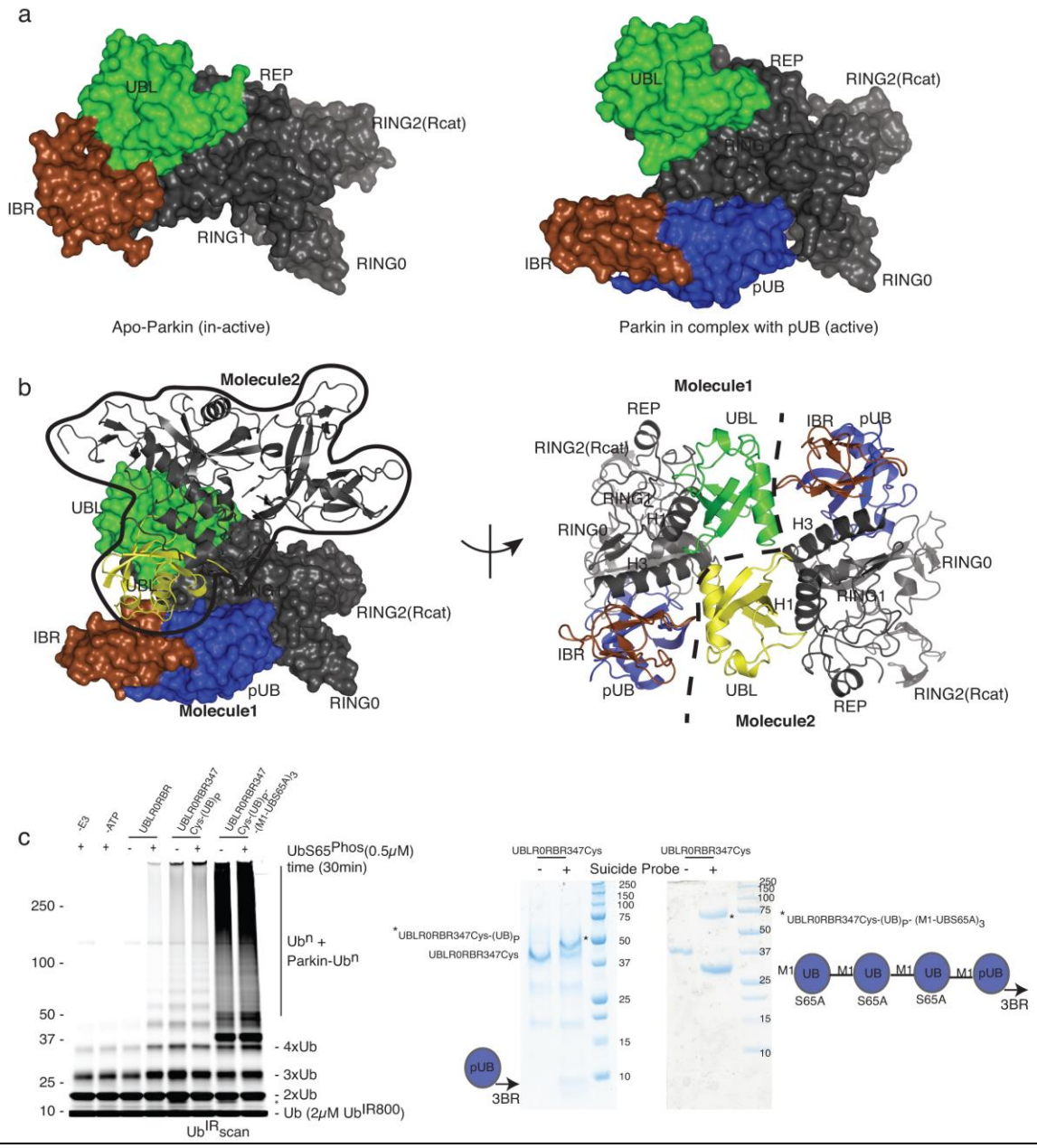

Supplementary Figure 2

Phosphoubiquitin binding to Parkin reveals cryptic ubiquitin binding sites

a) Comparison of apo structure of UBLR0RBR (left) with UBLR0RBR-pUb complex (right). The surface representation shows the void created between the IBR (brown) and UBL (green) domains upon phosphoubiquitin (blue) binding. For clarity the rest of Parkin is shown in grey, with domains labelled. **b**) The void created between IBR (brown) and UBL (green) is occupied by a symmetry related molecule 2 of Parkin, mediated by UBL (yellow) of the second molecule. The second Parkin molecule is outlined (left), with the rest of Parkin shown in grey for clarity. A second cartoon view related by a ~90^{o} rotation around the y-axis shows the UBL of molecule 2 (yellow) nestling between the UBL (green) and IBR (brown) of molecule 1. Phosphoubiquitin is shown in blue. The crystal symmetry axis between the two molecules is represented by a dashed line. **c)** Massive enhancement in ubiquitin chain formation and Parkin autoubiquitination activity of Parkin upon UBLR0RBRCys347 linkage with (M1-UbS65A)$_3$-pUb-3BR probe (left panel). UBLR0RBRCys347 reaction with suicide probes (pUb-3BR/(M1-UbS65A) $_3$-pUb-3BR) is shown (right panel), reacted species of UBLR0RBR347Cys with suicide probe is marked with *.

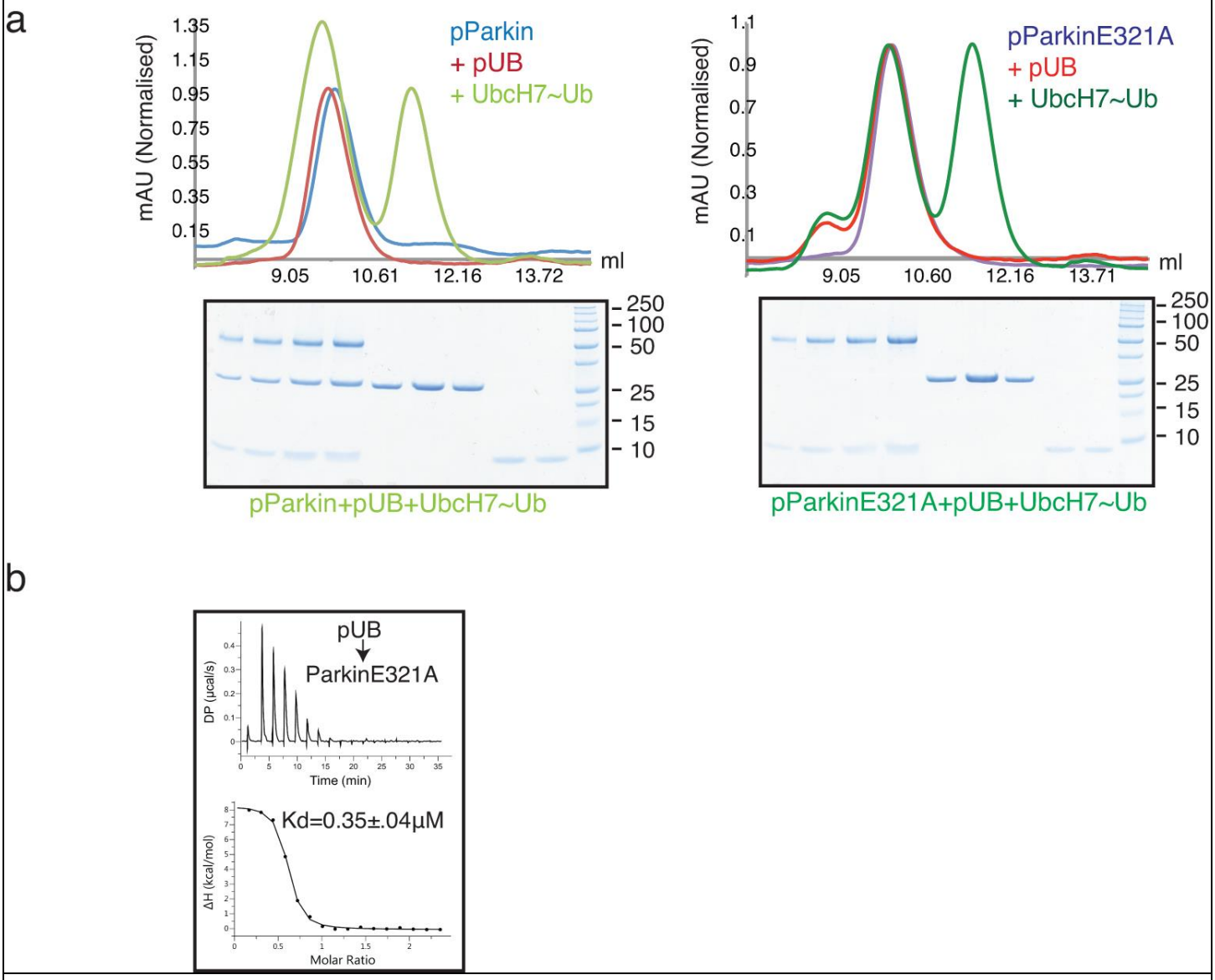

Supplementary Figure 3

Phosphoubiquitin binding enables recruitment of the charged E2, UbcH7~Ub

a) Size-exclusion chromatography of phosphoParkinE321A and pUb complex does not show any shift with UbcH7~Ub isopeptide, WT-phosphoParkin and pUb results in a shift and co-elutes with charged E2, fractions were confirmed by SDS PAGE analysis. **b**) Isothermal titration calorimetry shows that ParkinE321A associates with phosphoubiquitin with the same affinity as wild-type Parkin.

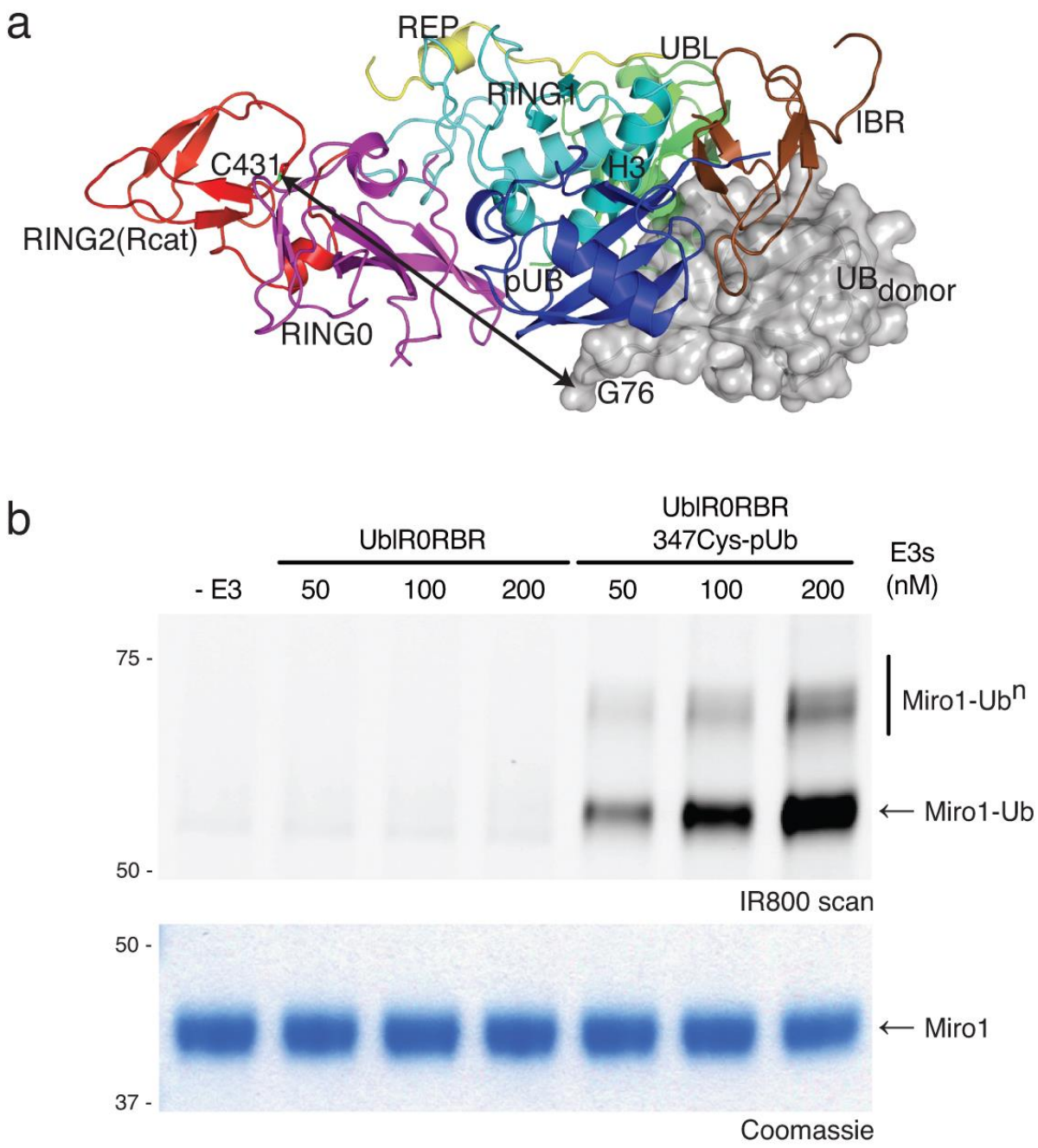

Supplementary Figure 4

Model of phosphoubiquitin-bound Parkin in complex with donor ubiquitin

a) The UblR0RBR structure in complex with phosphoubiquitin, coloured as in Figure 1a with all domains labelled, is modelled with a ubiquitin moiety in the H3-IBR binding site. The model is based on a combination of the crystallographically related UBL domain, the HOIP RBR/E2~Ub structure, and the chemical shift perturbations showing the ubiquitin binding site on Parkin. An arrow indicates the route from the tail of the ubiquitin molecule to the catalytic cysteine in the RING2(Rcat) domain. **b**) Ubiquitination assay following the ubiquitination of Miro1 in the presence of increasing concentrations of inactive UblR0RBR Parkin, or UblR0RBR covalently linked to phosphoubiquitin. Activity is monitored following fluorescently labelled ubiquitin, and a coomassie stained gel shows input levels.

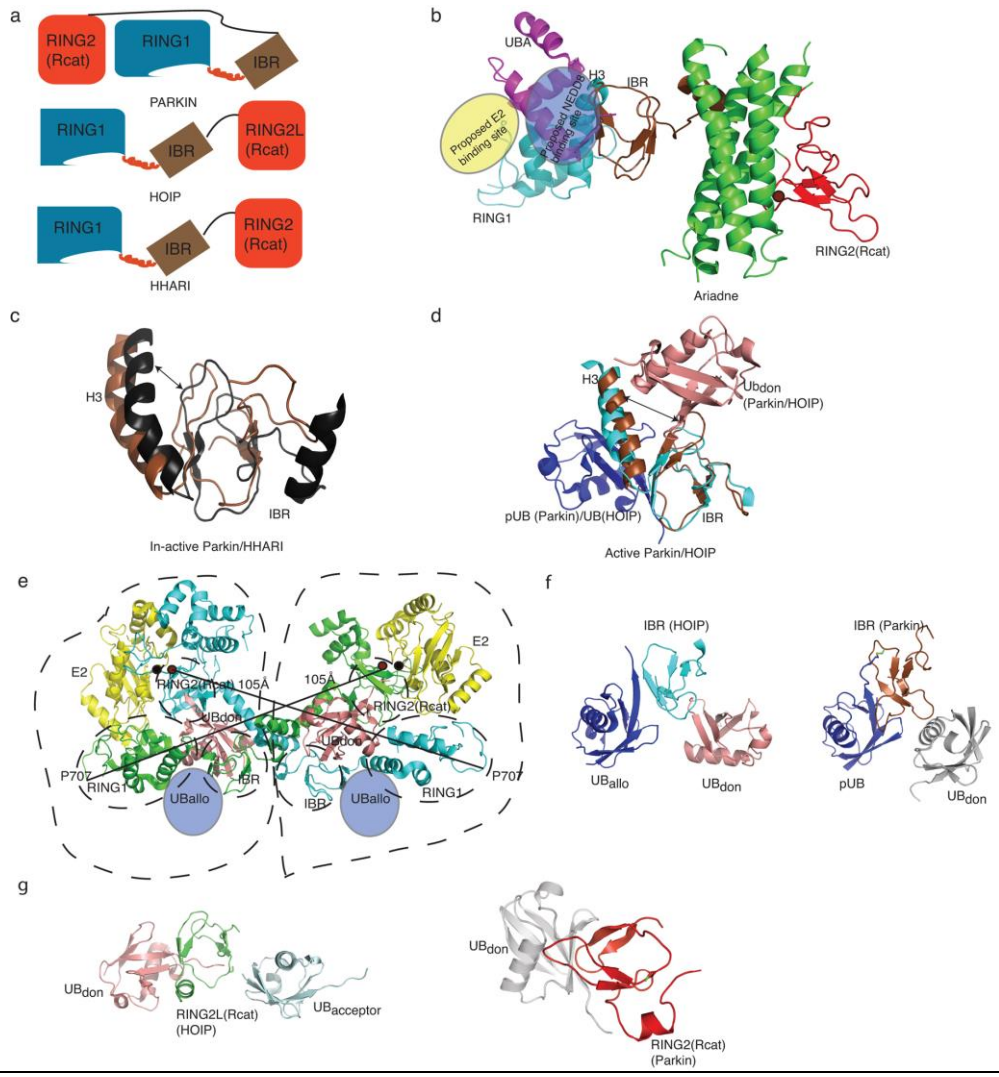

Supplementary Figure 5

Arrangements of domains in RBR modules suggests a common mode of regulation whereby the IBR and RING2(Rcat) of RBRs recruit multiple ubiquitin-like molecules

a) Structural arrangement of RING1-IBR-RING2(Rcat) Domain in Parkin (upper panel, pdb code 5C1Z), HOIP (middle panel, pdb code 4KBL), and HHARI (lower panel, pdb code 5EDV). **b)** Autoinhibited structure of HHARI (pdb code 4KBL), proposed E2 binding site and NEDD8 binding site are highlighted in yellow and blue circles, respectively. **c)** Superposition of H3-IBR of Parkin (brown, PDB code 5C1Z) and HHARI (black, PDB code 4KBL) in the autoinhibited state, compactness between helix (H3) and IBR is marked with an arrow. **d)** Superposition of H3-IBR of Parkin (brown, UBLR0RBR-pUb complex) and HOIP (cyan, PDB code: 5EDV) in the active state, with overlapping positions for activator ubiquitin (Ub_{allo} /pUb, blue) and donor ubiquitin (Ub_{don}, salmon red). **e)** Representation of the asymmetric unit of the crystal structure of HOIP in complex with E2~Ub and activator ubiquitin (Ub_{allo}) (pdb code 5EDV). The asymmetric unit contains two molecules of HOIP (green, cyan), E2 (yellow), donor ubiquitin (Ub_{don}, salmon), activator ubiquitin (Ub_{allo}, blue circle). RING1, IBR and RING2(Rcat) domains are circled with dashed line, distance between catalytic cysteine of RING2(Rcat), Cys885 (brown circle), and RING1 (P707) of the same molecule is represented by straight solid line. Catalytic cysteine, Cys86, of E2 is represented as black circle. Processive unit of HOIP (marked with dashed line) is formed by RING1-IBR from one molecule of HOIP, RING2(Rcat) from another molecule of HOIP interacting with E2, Ub_{don} and Ub_{allo}, **f)** IBR (cyan) of HOIP (pdb code 5EDV) interacting with activator ubiquitin (Ub_{allo}, blue) and donor ubiquitin (Ub_{don}, salmon red), left panel.IBR (brown) of Parkin (UBLR0RBR-pUb complex) interacting with pUb (blue) and donor ubiquitin (Ub_{don}, grey), right panel.**g)** RING2L/Rcat (cyan) of HOIP (pdb code 4LJP) interacting with donor ubiquitin (Ub_{don}, salmon red) and acceptor ubiquitin (pale cyan), left panel. RING2(Rcat) (brown) of Parkin (UBLR0RBR-pUb complex) interacting with donor ubiquitin (Ub_{don}, grey), right panel.